*Journal of Parasitology* 2020 106(1) 133–156
© American Society of Parasitologists 2020

Published 12 February 2020

Contents and archives available through www.bioone.org or www.jstor.org

# Journal of Parasitology

journal homepage: www.journalofparasitology.org

DOI: 10.1645/19-129

# FOUR NEW SPECIES OF *PARAORYGMATOBOTHRIUM* (EUCESTODA: PHYLLOBOTHRIIDEA) FROM SHARKS OF THE GULF OF MEXICO AND THE ATLANTIC OCEAN, WITH COMMENTS ON THEIR HOST SPECIFICITY

**T. R. Ruhnke[1], V. Daniel[1], and K. Jensen[2]**

[1] Department of Biology, Barron Drive, West Virginia State University, Institute, West Virginia 25112-1000.
[2] Department of Ecology and Evolutionary Biology and the Biodiversity Institute, 1200 Sunnyside Ave., University of Kansas, Lawrence, Kansas 66045.
Correspondence should be sent to T. R. Ruhnke at: *ruhnketr@wvstateu.edu*

**KEY WORDS**

*Paraorygmatobothrium*
Carcharhinidae
United States
Atlantic Ocean
*28S rDNA*
Phylogenetic Analysis
*COI*
Host Specificity

**ABSTRACT**

Four new species of *Paraorygmatobothrium* are described from carcharhinid shark species from the Gulf of Mexico and the U.S. coast of the northwestern Atlantic Ocean. *Paraorygmatobothrium bullardi* n. sp. is described from *Carcharhinus brevipinna* as its type host, and from *Carcharhinus acronotus* and *Carcharhinus limbatus*. *Paraorygmatobothrium campbelli* n. sp. is described from *Rhizoprionodon terraenovae*. *Paraorygmatobothrium deburonae* n. sp. is described from *Carcharhinus isodon* as its type host, as well as from *C. brevipinna*, *C. limbatus*, and *R. terraenovae*. *Paraorygmatobothrium mattisi* n. sp. is described from *R. terraenovae* as its type host, and from *C. brevipinna* and *C. limbatus*. These 4 species differ from other species of *Paraorygmatobothrium* and from each other in bothridial microthrix shape, and in various combinations of features such as the total length of the worm, apical sucker size, bothridial musculature, proglottid number, testes number, and genital pore position. Difficulty in differentiating these 4 species from one another, and from other species of *Paraorygmatobothrium*, points to limitations in the use of morphology alone to recognize species diversity in this genus. A phylogenetic analysis of *Paraorygmatobothrium* and related genera, based on partial (D1–D3) *28S rDNA* sequence data, confirms that the genus is not monophyletic. Genetic distances of *COI* revealed that sequence divergence between species of *Paraorygmatobothrium* is generally at least an order of magnitude larger than *COI* divergence within a species. Patterns of host use for 3 of the new species are consistent with previous findings that point to a lack of host specificity in *Paraorygmatobothrium*.

In a survey of larval and adult cestodes of the Gulf of Mexico, Jensen and Bullard (2010) collected adult specimens of 4 species of *Paraorygmatobothrium* Ruhnke, 1994, from carcharhinid sharks and referred to these species as *Paraorygmatobothrium* sp. 2, sp. 3, sp. 5, and sp. 6. Specimens of *Paraorygmatobothrium* sp. 2 were collected from the Atlantic sharpnose shark, *Rhizoprionodon terraenovae* (Richardson). Specimens of *Paraorygmatobothrium* sp. 3 were taken from the Spinner shark, *Carcharhinus brevipinna* (Müller and Henle), the Blacktip shark, *Carcharhinus limbatus* (Müller and Henle), and *R. terraenovae*. Specimens of *Paraorygmatobothrium* sp. 5 were taken from the Finetooth shark, *Carcharhinus isodon* (Müller and Henle), *C. brevipinna, C. limbatus*, and *R. terraenovae*. Last, specimens of *Paraorygmatobothrium* sp. 6 were taken from *C. brevipinna*. Jensen and Bullard (2010) did not provide morphological characterizations for these putative new species but provided evidence from partial (D1–D3) *28S rDNA* sequence data that these 4 species were phylogenetically distinct from one another. Morphological data and sequence data generated for additional specimens of these species of *Paraorygmatobothrium* from hosts collected by Jensen and Bullard (2010), as well as specimens collected from the same and additional carcharhinid shark species from elsewhere in the Gulf of Mexico and the northwestern Atlantic Ocean off Florida and South Carolina, confirmed these 4 species to not only be distinct from one another, but also distinct from all other species in the genus.

The purpose of this paper is to formally describe these 4 species, which includes details of the scolex and strobilar microthrix patterns, and to determine their phylogenetic placement among all existing species of *Paraorygmatobothrium* and closely related phyllobothriidean genera for which partial *28S rDNA* sequence data are available. Intra- and inter-specific variation in *COI* sequence data were used to support new species status.

Version of Record, first published online with fixed content and layout, in compliance with ICZN Arts. 8.1.3.2, 8.5, and 21.8.2 as amended, 2012. Zoobank publication registration: urn:lsid:zoobank.org:pub: 5C933085-6063-4E9C-A216-D67023E8486D

## MATERIALS AND METHODS

In total, tapeworms from 26 carcharhinid shark specimens were examined during this study: 1 specimen of the Blacknose shark, *Carcharhinus acronotus* (Poey) from the Gulf of Mexico off Florida (KC-5); 3 specimens of *C. brevipinna* from the Gulf of Mexico off Louisiana (MS05-357) and Mississippi (MS05-5, MS05-457); 5 specimens of *C. isodon* from the Gulf of Mexico off Florida (MS05-495, MS05-496) and Mississippi (MS05-83, MS05-86), and the Atlantic Ocean off South Carolina (CH-49); 11 specimens of *C. limbatus* from the Gulf of Mexico off Florida (MS05-435, MS05-482, MS05-484, MS05-488, MS05-489, MS05-490, MS05-491, KC-7) and Mississippi (MS05-24), and from the Atlantic Ocean off Florida (DEL-8) and South Carolina (CH-48); 6 specimens of *R. terraenovae* from the Gulf of Mexico off Florida (TM-1) and Mississippi (MS05-21, MS05-23, MS05-550), and from the Atlantic Ocean off Florida (DEL-13) and South Carolina (CH-8). For each, more detailed specimen and collection data can be accessed in the Global Cestode Database (http://elasmobranchs.tapewormdb.uconn.edu/; Caira et al., 2018) by searching on the Collection Code and Collection Number (e.g., MS05-21) assigned to each specimen. Tapeworm specimens were collected and processed from these sharks via methods given in either Jensen and Bullard (2010) or Ruhnke and Workman (2013).

Formalin-fixed specimens, including hologenophores and paragenophores (sensu Pleijel et al., 2008), were prepared as whole mounts following the methods given in Ruhnke and Workman (2013). Specimens for scanning electron microscopy were prepared following the methods given in Herzog and Jensen (2017). Specimens were examined with a Hitachi SU8320 Cold Field Emission scanning electron microscope at the Microscopy Analytical Imaging Resource Core Laboratory, University of Kansas, Lawrence, Kansas. Illustrations were made with the aid of a camera lucida attached to a Zeiss Axioskop 2 (Carl Zeiss, Inc., Thornwood, New York). Measurements are given as the range, followed in parentheses by the mean, standard deviation, number of worms measured, and total number of measurements if more than 1 measurement per worm was taken. Measurements are reported in micrometers unless otherwise stated. Microthrix terminology follows Chervy (2009).

Hologenophore specimens of the 4 new species used in Jensen and Bullard (2010) were borrowed from the Lawrence R. Penner Parasitology Collection, University of Connecticut. Museum abbreviations used are as follows: LRP, Lawrence R. Penner Parasitology Collection, Department of Ecology and Evolutionary Biology, University of Connecticut, Storrs, Connecticut; and USNM, United States National Museum, Smithsonian Institution, Washington, D.C.

For the phylogenetic analysis, sequence data for partial (D1–D3) *28S rDNA* were generated de novo in this study for 3 to 7 specimens of each of the new species of *Paraorygmatobothrium* described herein. In addition, novel sequence data were generated for 4 specimens of *Paraorygmatobothrium arnoldi* Ruhnke and Thompson, 2006; 3 specimens of *Paraorygmatobothrium typicum* (Subhapradha, 1955) Ruhnke, 2011; 2 specimens each of *Paraorygmatobothrium janineae* Ruhnke, Healy, and Shapero, 2006 and *Paraorygmatobothrium exiguum* (Yamaguti, 1935) Ruhnke, 1994; and 1 specimen each of *Paraorygmatobothrium prionacis* (Yamaguti, 1934) Ruhnke, 1994, *Paraorygmatobothrium paulum* (Linton, 1897) Ruhnke, 2011, and *Paraorygmatobothrium christopheri* Cutmore, Bennett, Miller, and Cribb, 2017. Total genomic DNA was extracted using the Qiagen DNEasy Blood and Tissue Kit (Qiagen, Germantown, Maryland) with alterations made to the kit protocol as given in Ruhnke et al. (2015). Partial (D1–D3) *28S rDNA* was amplified using ProMega GoTaq Green PCR master mix (Promega, Madison, Wisconsin) in a total reaction volume of 25 µl. For DNA templates that proved difficult to amplify, ProMega GoTaq Green HotStart PCR master mix (Promega) was used in the place of the normal master mix. The primer combinations used for *28S rDNA* amplification were selected from those given in Ruhnke and Workman (2013). The thermocycler temperature profile for the *28S rDNA* reaction was an initial incubation at 95 C for 2 min, denaturation at 95 C for 30 sec, annealing at 52 C for 30 sec, and extension at 72 C for 1 min and 30 sec for 40–45 cycles. The reaction was completed by a 5-min incubation at 72 C and then held indefinitely at 10 C. The PCR amplicons were visualized using gel electrophoresis following the protocols given in Ruhnke et al. (2015), with the exception of using 70 ml 1× TBE buffer instead of 70 ml 1× TAE buffer and using 7 µl of Phenix GelRed stain (Phenix Research, Candler, North Carolina) instead of 3 µl of ethidium bromide. Gel purification was achieved using a ProMega Wizard SV Gel and PCR Clean-Up System (Promega). The kit protocol was followed with 1 exception: Final incubation time with elution buffer was extended from 1 min to 15–30 min. Gel electrophoresis was conducted to assess which amplicons were suitable for sequencing. DNA was sequenced using ABI Big Dye (Applied Biosystems, Foster City, California) chemistry; sequencing products were cleaned using either EDTA/ethanol precipitation or Sephadex (GE Healthcare Life Sciences, Pittsburgh, Pennsylvania), and products were analyzed in an ABI 3130xl genetic analyzer (Applied Biosystems). Contiguous sequences were assembled in Geneious v. 10.1.3 (Biomatters, Newark, New Jersey).

Partial (D1–D3) *28S rDNA* sequence data generated for the 34 specimens of *Paraorygmatobothrium* de novo were combined with 32 of the 33 sequences of adult specimens of *Paraorygmatobothrium* from Jensen and Bullard (2010), and 38 sequences of *Paraorygmatobothrium* and allied phyllobothriidean species generated by Ruhnke and Workman (2013), Caira et al. (2014), and Cutmore et al. (2011, 2017), available in GenBank (Benson et al., 2005). Representatives of the phyllobothriidean genera *Alexandercestus* Ruhnke and Workman, 2013; *Hemipristicola* Cutmore, Theiss, Bennett, and Cribb, 2011; and *Thysanocephalum* Linton, 1890, were chosen as outgroups informed by the phylogenetic analyses of Cutmore et al. (2017). The sequence data for the 2 specimens of *Alexandercestus* generated by Ruhnke and Workman (2013) and Cutmore et al. (2017), and for the 1 specimen of *Thysanocephalum thysanocephalum* (Linton, 1889) Braun, 1900 generated by Caira et al. (2014) were available in GenBank; sequence data for *Hemipristicola gunterae* Cutmore, Theiss, Bennett, and Cribb, 2011 were generated de novo. Voucher accession numbers (for hologenophores, or, in 3 instances, photo vouchers), GenBank numbers, and host accession numbers, specimen IDs, as well as host species and localities for all specimens for which *28S rDNA* sequence data were generated are given in Table I.

Sequences of the 104 ingroup specimens and 4 outgroup specimens were assembled into a matrix and trimmed in Geneious

Table I. List of taxa included in the phylogenetic analysis with their specimen, voucher, host, and locality data. GenBank numbers in bold indicate sequences generated as part of this study.

| Ingroup/ Outgroup | Taxon | Specimen ID | Voucher accession no.* | GenBank accession no. (*28S rDNA*) | GenBank accession no. (*COI*) | Host accession no.† | Host species | Locality | Source |
|---|---|---|---|---|---|---|---|---|---|
| Outgroup | *Alexandercestus gibsoni* Ruhnke and Workman, 2013 | PEET 242 | LRP 7957 | KC505623 | N/A | AU-30 | *Negaprion acutidens* (Rüppell) | Timor Sea, Northern Territory, Australia | Ruhnke and Workman (2013) |
| Outgroup | *A. gibsoni* | | QM G232747 | MG008925 | N/A | | *Carcharhinus leucas* Müller and Henle | western Moreton Bay, Queensland, Australia | Cutmore et al. (2017) |
| Outgroup | *Hemipristicola gunterae* Cutmore, Theiss, Bennett, and Cribb, 2011 | PEET 470 | LRP 10051 | **MN686526** | N/A | NT-67 | *Hemipristis elongata* (Klunzinger) | east of Wessel Islands (11°17′44″S, 136°59′48″E), Arafura Sea, Northern Territory, Australia | this study |
| Outgroup | *Thysanocephalum thysanocephalum* (Linton, 1889) Braun, 1900 | TE-43B | LRP 8290 | KF685902 | N/A | KC-13 | *Galeocerdo cuvier* Péron and Lesueur | Atlantic Ocean, South Carolina | Caira et al. (2014) |
| Ingroup | *Doliobothrium* sp. | | QM G232937 | MG008928 | | | *Rhizoprionodon taylori* (Ogilby) | western Moreton Bay, Queensland, Australia | Cutmore et al. (2017) |
| Ingroup | *Doliobothrium* sp. | | QM G232942 | MG008929 | | | *Sphyrna lewini* (Griffith and Smith) | western Moreton Bay, Queensland, Australia | Cutmore et al. (2017) |
| Ingroup | *Marsupiobothrium* sp. 1 | | LRP 8337 | KF685771 | | BJ-719 | *Alopias pelagicus* Nakamura | Santa Rosalia, Baja California Sur, Mexico | Caira et al. (2014) |
| Ingroup | *Nandocestus guariticus* (Marques, Brooks, and Lasso, 2001) Reyda, 2008 | TE-34A | LRP 8286 | KF685888 | | PU-15 | *Paratrygon aiereba* (Müller and Henle) | Madre de Dios, Peru | Caira et al. (2014) |
| Ingroup | *Orectolobicestus tyleri* Ruhnke, Caira, and Carpenter, 2006 | | QM G232868 | MG008930 | | | *Chiloscyllium* cf. *punctatum* Müller and Henle | western Moreton Bay, Queensland, Australia | Cutmore et al. (2017) |
| Ingroup | *O. tyleri* | TE-101 | LRP 8315 | KF685890 | | BO-472 | *C. punctatum* | Mukah, Sarawak, Malaysia | Caira et al. (2014) |
| Ingroup | *Orectolobicestus randyi* Ruhnke, Caira, and Carpenter, 2006 | TE-105 | LRP 8318 | KF685767 | | BO-493 | *Chiloscyllium hasseltii* Bleeker | Mukah, Sarawak, Malaysia | Caira et al. (2014) |
| Ingroup | *Paraorygmatobothrium arnoldi* Ruhnke and Thompson, 2006 | PEET 492 | LRP 10052 | **MN686527** | **MN659388** | CM03-66 | *N. acutidens* | Weipa (12°35′11″S, 141°42′34″E), Queensland, Australia | this study |
| Ingroup | *P. arnoldi* | PEET 333 | LRP 10053 | **MN686528** | **MN659389** | CM03-68 | *N. acutidens* | Weipa (12°35′11″S, 141°42′34″E), Queensland, Australia | this study |
| Ingroup | *P. arnoldi* | PEET 334 | LRP 10054 | **MN686529** | | CM03-68 | *N. acutidens* | Weipa (12°35′11″S, 141°42′34″E), Queensland, Australia | this study |
| Ingroup | *P. arnoldi* | PEET 372 | LRP 10055‡ | **MN686530** | | CM03-66 | *N. acutidens* | Weipa (12°35′11″S, 141°42′34″E), Queensland, Australia | this study |

Table I. Continued.

| Ingroup/ Outgroup | Taxon | Specimen ID | Voucher accession no.* | GenBank accession no. (*28S rDNA*) | GenBank accession no. (*COI*) | Host accession no.† | Host species | Locality | Source |
|---|---|---|---|---|---|---|---|---|---|
| Ingroup | *P. arnoldi* | PEET 115 | LRP 10056 | | **MN659390** | AU-82 | *N. acutidens* | Fog Bay (12°45′33″S, 130°21′7″E), Timor Sea, Northern Territory, Australia | this study |
| Ingroup | *Paraorygmatobothrium bai* Ruhnke and Carpenter, 2008 | PEET 94V | LRP 7960 | KC505625 | | SE-43 | *Mustelus mustelus* Linnaeus | Ouakam (14°42′54″N, 17°29′28″W), Senegal | Ruhnke and Workman (2013) |
| Ingroup | *P. bai* | PEET 132 | LRP 10057§ | | **MN659391** | SE-43 | *M. mustelus* | Ouakam (14°42′54″N, 17°29′28″W), Senegal | this study |
| Ingroup | *P. bai* | PEET 464 | LRP 10059 | | **MN659392** | SE-43 | *M. mustelus* | Ouakam (14°42′54″N, 17°29′28″W), Senegal | this study |
| Ingroup | *Paraorygmatobothrium bullardi* n. sp. | PEET 367 | LRP 10067 | **MN686531** | | KC-5 | *Carcharhinus acronotus* Poey | ~100 mi south of Tallahassee (28°37.15′N, 84°12.81′W), Gulf of Mexico, Florida | this study |
| Ingroup | *P. bullardi* n. sp. | PEET 382 | LRP 10069 | **MN686533** | **MN659393** | MS05-5 | *Carcharhinus brevipinna* Müller and Henle | south of Shallow Fields (29°37′22.8″N, 88°30′11″W), Gulf of Mexico, Mississippi | this study |
| Ingroup | *P. bullardi* n. sp. | PEET 465 | LRP 10070 | **MN686534** | **MN659394** | MS05-5 | *C. brevipinna* | south of Shallow Fields (29°37′22.8″N, 88°30′11″W), Gulf of Mexico, Mississippi | this study |
| Ingroup | *P. bullardi* n. sp. | PEET 467 | LRP 10071 | **MN686535** | | DEL-8 | *Carcharhinus limbatus* Müller and Henle | off Central Florida (28°0.8′N, 80°27′W), Atlantic Ocean | this study |
| Ingroup | *P. bullardi* n. sp. | PEET 381 | LRP 10068 | **MN686532** | | MS05-5 | *C. brevipinna* | south of Shallow Fields (29°37′22.8″N, 88°30′11″W), Gulf of Mexico, Mississippi | this study |
| Ingroup | *P. bullardi* n. sp. (as *P.* sp. 6 in Jensen and Bullard, 2010) | MS05-5-5 | LRP 7146 | GQ470001 | **MN659395** | MS05-5 | *C. brevipinna* | south of Shallow Fields (29°37′22.8″N, 88°30′11″W), Gulf of Mexico, Mississippi | Jensen and Bullard (2010) |
| Ingroup | *P. bullardi* n. sp. (as *P.* sp. 6 in Jensen and Bullard, 2010) | MS05-5-6 | LRP 7147 | GQ470002 | **MN659396** | MS05-5 | *C. brevipinna* | south of Shallow Fields (29°37′22.8″N, 88°30′11″W), Gulf of Mexico, Mississippi | Jensen and Bullard (2010) |
| Ingroup | *P. bullardi* n. sp. (as *P.* sp. 6 in Jensen and Bullard, 2010) | MS05-5-7 | LRP 7148 | GQ470003 | **MN659397** | MS05-5 | *C. brevipinna* | south of Shallow Fields (29°37′22.8″N, 88°30′11″W), Gulf of Mexico, Mississippi | Jensen and Bullard (2010) |
| Ingroup | *P. bullardi* n. sp. (as *P.* sp. 6 in Jensen and Bullard, 2010) | MS05-5-8 | LRP 7149 | GQ470004 | **MN659398** | MS05-5 | *C. brevipinna* | south of Shallow Fields (29°37′22.8″N, 88°30′11″W), Gulf of Mexico, Mississippi | Jensen and Bullard (2010) |
| Ingroup | *Paraorygmatobothrium campbelli* n. sp. | PEET 505 | LRP 10081 | **MN686538** | | DEL-13 | *Rhizoprionodon terraenovae* (Richardson) | off Florida (29°35.38′N, 80°32.3′W), Atlantic Ocean | this study |
| Ingroup | *P. campbelli* n. sp. | PEET 504 | LRP 10080 | **MN686537** | | DEL-13 | *R. terraenovae* | off Florida (29°35.38′N, 80°32.3′W), Atlantic Ocean | this study |

Table I. Continued.

| Ingroup/ Outgroup | Taxon | Specimen ID | Voucher accession no.* | GenBank accession no. (*28S rDNA*) | GenBank accession no. (*COI*) | Host accession no.† | Host species | Locality | Source |
|---|---|---|---|---|---|---|---|---|---|
| Ingroup | *P. campbelli* n. sp. | PEET 480 | LRP 10079 | **MN686536** | **MN659399** | CH-8 | *R. terraenovae* | Wadmalaw Point (32°37′45.84″N, 80°16′02.26″W), North Edisto River, Atlantic Ocean, South Carolina | this study |
| Ingroup | *P. campbelli* n. sp. (as *P.* sp. 2 in Jensen and Bullard, 2010) | MS05-23-3 | LRP 7189 | GQ470020 | **MN659400** | MS05-23 | *R. terraenovae* | Horn Island (30°14′37.70″N, 88°46′37.62″W), Gulf of Mexico, Mississippi | Jensen and Bullard (2010) |
| Ingroup | *P. campbelli* n. sp. (as *P.* sp. 2 in Jensen and Bullard, 2010) | MS05-23-4 | LRP 7190 | GQ470021 | **MN659401** | MS05-23 | *R. terraenovae* | Horn Island (30°14′37.70″N, 88°46′37.62″W), Gulf of Mexico, Mississippi | Jensen and Bullard (2010) |
| Ingroup | *P. campbelli* n. sp. (as *P.* sp. 2 in Jensen and Bullard, 2010) | MS05-23-5 | LRP 7191 | GQ470023 | **MN659402** | MS05-23 | *R. terraenovae* | Horn Island (30°14′37.70″N, 88°46′37.62″W), Gulf of Mexico, Mississippi | Jensen and Bullard (2010) |
| Ingroup | *P. campbelli* n. sp. (as *P.* sp. 2 in Jensen and Bullard, 2010) | MS05-23-6 | LRP 7192 | GQ470024 | **MN659403** | MS05-23 | *R. terraenovae* | Horn Island (30°14′37.70″N, 88°46′37.62″W), Gulf of Mexico, Mississippi | Jensen and Bullard (2010) |
| Ingroup | *Paraorygmatobothrium christopheri* Cutmore, Bennett, Miller, and Cribb, 2017 | | QM G233225 | MG008931 | | | *Carcharhinus sorrah* Müller and Henle | western Moreton Bay, Queensland, Australia | Cutmore et al. (2017) |
| Ingroup | *P. christopheri* | PEET 345 | LRP 10082 | **MN686539** | **MN659404** | NT-17 | *C.* cf. *sorrah* | Nhulunbuy, Northern Territory, Australia | this study |
| Ingroup | *P. christopheri* | PEET 544 | LRP 10084 | | **MN659405** | NT-53 | *Carcharhinus coatsi* Whitely | east of Wessel Islands (11°17′44″S, 136°59′48″E), Arafura Sea, Northern Territory, Australia | this study |
| Ingroup | *Paraorygmatobothrium deburonae* n. sp. | PEET 164 | LRP 10100 | | **MN659406** | MS05-83 | *Carcharhinus isodon* Müller and Henle | Round Island (30°17′42.45″N, 88°35′11.55″W), Gulf of Mexico, Mississippi | this study |
| Ingroup | *P. deburonae* n. sp. | PEET 385 | LRP 10095 | **MN686542** | **MN659407** | MS05-489 | *C. limbatus* | Indian Pass (29°40′8.05″N, 85°13′30.17″W), Gulf of Mexico, Florida | this study |
| Ingroup | *P. deburonae* n. sp. | PEET 379 | LRP 10093 | **MN686540** | | MS05-495 | *C. isodon* | Indian Pass (29°40′8.05″N, 85°13′30.17″W), Gulf of Mexico, Florida | this study |
| Ingroup | *P. deburonae* n. sp. | PEET 380 | LRP 10094 | **MN686541** | | MS05-495 | *C. isodon* | Indian Pass (29°40′8.05″N, 85°13′30.17″W), Gulf of Mexico, Florida | this study |
| Ingroup | *P. deburonae* n. sp. | PEET 444 | LRP 10096 | **MN686543** | **MN659408** | MS05-488 | *C. limbatus* | Indian Pass (29°40′8.05″N, 85°13′30.17″W), Gulf of Mexico, Florida | this study |
| Ingroup | *P. deburonae* n. sp. | PEET 483 | LRP 10097 | **MN686544** | **MN659409** | CH-48 | *C. limbatus* | Bulls Bay, Atlantic Ocean, South Carolina | this study |

Table I. Continued.

| Ingroup/ Outgroup | Taxon | Specimen ID | Voucher accession no.* | GenBank accession no. (*28S rDNA*) | GenBank accession no. (*COI*) | Host accession no.† | Host species | Locality | Source |
|---|---|---|---|---|---|---|---|---|---|
| Ingroup | *P. deburonae* n. sp. | PEET 484 | LRP 10098 | **MN686545** | **MN659410** | CH-49 | *C. isodon* | Bulls Bay, Atlantic Ocean, South Carolina | this study |
| Ingroup | *P. deburonae* n. sp. | PEET 485 | LRP 10099 | **MN686546** | **MN659411** | CH-49 | *C. isodon* | Bulls Bay, Atlantic Ocean, South Carolina | this study |
| Ingroup | *P. deburonae* n. sp. (as *P.* sp. 5A in Jensen and Bullard, 2010) | MS05-4-1 | LRP 7144 | GQ470031 | **MN659412** | MS05-4 | *C. brevipinna* | south of Shallow Fields (29°37.38″N, 88°30′11″W), Gulf of Mexico, Mississippi | Jensen and Bullard (2010) |
| Ingroup | *P. deburonae* n. sp. (as *P.* sp. 5A in Jensen and Bullard, 2010) | MS05-4-2 | LRP 7145 | GQ470032 | **MN659413** | MS05-4 | *C. brevipinna* | south of Shallow Fields (29°37.38″N, 88°30′11″W), Gulf of Mexico, Mississippi | Jensen and Bullard (2010) |
| Ingroup | *P. deburonae* n. sp. (as *P.* sp. 5D in Jensen and Bullard, 2010) | MS05-21-4 | LRP 7196 | GQ470048 | **MN659425** | MS05-21 | *R. terraenovae* | Horn Island (30°14′37.70″N, 88°46′37.62″W), Gulf of Mexico, Mississippi | Jensen and Bullard (2010) |
| Ingroup | *P. deburonae* n. sp. (as *P.* sp. 5D in Jensen and Bullard, 2010) | MS05-21-7 | LRP 7197 | GQ470033 | **MN659426** | MS05-21 | *R. terraenovae* | Horn Island (30°14′37.70″N, 88°46′37.62″W), Gulf of Mexico, Mississippi | Jensen and Bullard (2010) |
| Ingroup | *P. deburonae* n. sp. (as *P.* sp. 5D in Jensen and Bullard, 2010) | MS05-21-8 | LRP 7198 | GQ470046 | **MN659427** | MS05-21 | *R. terraenovae* | Horn Island (30°14′37.70″N, 88°46′37.62″W), Gulf of Mexico, Mississippi | Jensen and Bullard (2010) |
| Ingroup | *P. deburonae* n. sp. (as *P.* sp. 5C in Jensen and Bullard, 2010) | MS05-24-6 | LRP 7174 | GQ470034 | **MN659421** | MS05-24 | *C. limbatus* | Horn Island (30°14′37.70″N, 88°46′37.62″W), Gulf of Mexico, Mississippi | Jensen and Bullard (2010) |
| Ingroup | *P. deburonae* n. sp. (as *P.* sp. 5C in Jensen and Bullard, 2010) | MS05-24-7 | LRP 7175 | GQ470035 | **MN659422** | MS05-24 | *C. limbatus* | Horn Island (30°14′37.70″N, 88°46′37.62″W), Gulf of Mexico, Mississippi | Jensen and Bullard (2010) |
| Ingroup | *P. deburonae* n. sp. (as *P.* sp. 5C in Jensen and Bullard, 2010) | MS05-24-9 | LRP 7176 | GQ470036 | | MS05-24 | *C. limbatus* | Horn Island (30°14′37.70″N, 88°46′37.62″W), Gulf of Mexico, Mississippi | Jensen and Bullard (2010) |
| Ingroup | *P. deburonae* n. sp. (as *P.* sp. 5C in Jensen and Bullard, 2010) | MS05-24-10 | LRP 7177 | | **MN659423** | MS05-24 | *C. limbatus* | Horn Island (30°14′37.70″N, 88°46′37.62″W), Gulf of Mexico, Mississippi | Jensen and Bullard (2010) |
| Ingroup | *P. deburonae* n. sp. (as *P.* sp. 5C in Jensen and Bullard, 2010) | MS05-24-11 | LRP 7178 | GQ470047 | **MN659424** | MS05-24 | *C. limbatus* | Horn Island (30°14′37.70″N, 88°46′37.62″W), Gulf of Mexico, Mississippi | Jensen and Bullard (2010) |
| Ingroup | *P. deburonae* n. sp. (as *P.* sp. 5B in Jensen and Bullard, 2010) | MS05-83-4 | LRP 7158 | GQ470039 | **MN659414** | MS05-83 | *C. isodon* | Round Island (30°17′42.45″N, 88°35′11.55″W), Gulf of Mexico, Mississippi | Jensen and Bullard (2010) |
| Ingroup | *P. deburonae* n. sp. (as *P.* sp. 5B in Jensen and Bullard, 2010) | MS05-83-5 | LRP 7159 | GQ470041 | **MN659415** | MS05-83 | *C. isodon* | Round Island (30°17′42.45″N, 88°35′11.55″W), Gulf of Mexico, Mississippi | Jensen and Bullard (2010) |
| Ingroup | *P. deburonae* n. sp. (as *P.* sp. 5B in Jensen and Bullard, 2010) | MS05-83-6 | LRP 7160 | GQ470037 | **MN659416** | MS05-83 | *C. isodon* | Round Island (30°17′42.45″N, 88°35′11.55″W), Gulf of Mexico, Mississippi | Jensen and Bullard (2010) |

Table I. Continued.

| Ingroup/ Outgroup | Taxon | Specimen ID | Voucher accession no.* | GenBank accession no. (*28S rDNA*) | GenBank accession no. (*COI*) | Host accession no.† | Host species | Locality | Source |
|---|---|---|---|---|---|---|---|---|---|
| Ingroup | *P. deburonae* n. sp. (as *P.* sp. 5B in Jensen and Bullard, 2010) | MS05-83-7 | LRP 7161 | GQ470044 | **MN659417** | MS05-83 | *C. isodon* | Round Island (30°17′42.45″N, 88°35′11.55″W), Gulf of Mexico, Mississippi | Jensen and Bullard (2010) |
| Ingroup | *P. deburonae* n. sp. (as *P.* sp. 5B in Jensen and Bullard, 2010) | MS05-83-8 | LRP 7162 | GQ470043 | **MN659418** | MS05-83 | *C. isodon* | Round Island (30°17′42.45″N, 88°35′11.55″W), Gulf of Mexico, Mississippi | Jensen and Bullard (2010) |
| Ingroup | *P. deburonae* n. sp. (as *P.* sp. 5B in Jensen and Bullard, 2010) | MS05-83-9 | LRP 7163 | GQ470042 | **MN659419** | MS05-83 | *C. isodon* | Round Island (30°17′42.45″N, 88°35′11.55″W), Gulf of Mexico, Mississippi | Jensen and Bullard (2010) |
| Ingroup | *P. deburonae* n. sp. (as *P.* sp. 5B in Jensen and Bullard, 2010) | MS05-86-1 | LRP 7164 | GQ470038 | | MS05-86 | *C. isodon* | Round Island (30°17′42.45″N, 88°35′11.55″W), Gulf of Mexico, Mississippi | Jensen and Bullard (2010) |
| Ingroup | *P. deburonae* n. sp. (as *P.* sp. 5B in Jensen and Bullard, 2010) | MS05-86-2 | LRP 7165 | GQ470040 | **MN659420** | MS05-86 | *C. isodon* | Round Island (30°17′42.45″N, 88°35′11.55″W), Gulf of Mexico, Mississippi | Jensen and Bullard (2010) |
| Ingroup | *Paraorygmatobothrium exiguum* (Yamaguti, 1935) Ruhnke, 1994 | PEET 456 | LRP 10101‡ | **MN686547** | **MN659428** | AI-29 | *Alopias vulpinus* Bonnaterre | off Montauk, Long Island Sound, New York | this study |
| Ingroup | *P. exiguum* | PEET 457 | LRP 10102 | **MN686548** | **MN659429** | AI-29 | *A. vulpinus* | off Montauk, Long Island Sound, New York | this study |
| Ingroup | *P. exiguum* | TE-98 | LRP 8313 | KF685769 | | TK-1 | *A. vulpinus* | off Montauk, Long Island Sound, New York | Caira et al. (2014) |
| Ingroup | *Paraorygmatobothrium harti* Cutmore, Bennett, Miller, and Cribb, 2017 | | QM G233258 | MG008939 | | | *C. leucas* | Brisbane River, Queensland, Australia | Cutmore et al. (2017) |
| Ingroup | *Paraorygmatobothrium janineae* Ruhnke, Healy, and Shapero, 2006 | PEET 458 | LRP 10103 | **MN686549** | | NT-67 | *H. elongata* | east of Wessel Islands (11°17′44″S, 136°59′48″E), Arafura Sea, Northern Territory, Australia | this study |
| Ingroup | *P. janineae* | PEET 460 | LRP 10104 | **MN686550** | **MN659430** | NT-93 | *H. elongata* | east of Wessel Islands (11°17′44″S, 136°59′48″E), Arafura Sea, Northern Territory, Australia | this study |
| Ingroup | *P. janineae* | | hologenophore not deposited | HQ680625 | | | *H. elongata* | Wynnum banks, Moreton Bay, Queensland, Australia | Cutmore et al. (2011) |
| Ingroup | *P. janineae* | | hologenophore not deposited | HQ680626 | | | *H. elongata* | Wynnum banks, Moreton Bay, Queensland, Australia | Cutmore et al. (2011) |
| Ingroup | *P. janineae* | | hologenophore not deposited | HQ680627 | | | *H. elongata* | Wynnum banks, Moreton Bay, Queensland, Australia | Cutmore et al. (2011) |
| Ingroup | *Paraorygmatobothrium kirstenae* Ruhnke, Healy, and Shapero, 2006 | PEET 223 | LRP 7962 | KC505626 | | BO-36 | *Hemigaleus microstoma* Bleeker | Mukah, Sarawak, Malaysia | Ruhnke and Workman (2013) |

Table I. Continued.

| Ingroup/ Outgroup | Taxon | Specimen ID | Voucher accession no.* | GenBank accession no. (*28S rDNA*) | GenBank accession no. (*COI*) | Host accession no.† | Host species | Locality | Source |
|---|---|---|---|---|---|---|---|---|---|
| Ingroup | *Paraorygmatobothrium mattisi* n. sp. (as *P.* sp. 3C in Jensen and Bullard, 2010) | MS05-21-3 | LRP 7193 | GQ470009 | **MN659433** | MS05-21 | *R. terraenovae* | Horn Island (30°14′37.70″N, 88°46′37.62″W), Gulf of Mexico, Mississippi | Jensen and Bullard (2010) |
| Ingroup | *P. mattisi* n. sp. (as *P.* sp. 3C in Jensen and Bullard, 2010) | MS05-21-5 | LRP 7194 | GQ470013 | **MN659434** | MS05-21 | *R. terraenovae* | Horn Island (30°14′37.70″N, 88°46′37.62″W), Gulf of Mexico, Mississippi | Jensen and Bullard (2010) |
| Ingroup | *P. mattisi* n. sp. (as *P.* sp. 3C in Jensen and Bullard, 2010) | MS05-21-6 | LRP 7195 | GQ470006 | **MN659435** | MS05-21 | *R. terraenovae* | Horn Island (30°14′37.70″N, 88°46′37.62″W), Gulf of Mexico, Mississippi | Jensen and Bullard (2010) |
| Ingroup | *P. mattisi* n. sp. (as *P.* sp. 3B in Jensen and Bullard, 2010) | MS05-24-8 | LRP 7172 | GQ470005 | **MN659431** | MS05-24 | *C. limbatus* | Horn Island (30°14′37.70″N, 88°46′37.62″W), Gulf of Mexico, Mississippi | Jensen and Bullard (2010) |
| Ingroup | *P. mattisi* n. sp. (as *P.* sp. 3B in Jensen and Bullard, 2010) | MS05-24-12 | LRP 7173 | GQ470007 | **MN659432** | MS05-24 | *C. limbatus* | Horn Island (30°14′37.70″N, 88°46′37.62″W), Gulf of Mexico, Mississippi | Jensen and Bullard (2010) |
| Ingroup | *P. mattisi* n. sp. (as *P.* sp. 3A in Jensen and Bullard, 2010) | MS05-457-1 | LRP 7142 | GQ470011 | | MS05-457 | *C. brevipinna* | Horn Island (30°14′37.70″N, 88°46′37.62″W), Gulf of Mexico, Mississippi | Jensen and Bullard (2010) |
| Ingroup | *P. mattisi* n. sp. (as *P.* sp. 3A in Jensen and Bullard, 2010) | MS05-457-2 | LRP 7143 | GQ470012 | | MS05-457 | *C. brevipinna* | Horn Island (30°14′37.70″N, 88°46′37.62″W), Gulf of Mexico, Mississippi | Jensen and Bullard (2010) |
| Ingroup | *P. mattisi* n. sp. | PEET 384 | LRP 10113 | **MN686551** | | MS05-488 | *C. limbatus* | Indian Pass (29°40′8.05″N, 85°13′30.17″W), Gulf of Mexico, Florida | this study |
| Ingroup | *P. mattisi* n. sp. | PEET 386 | LRP 10114 | **MN686552** | | MS05-490 | *C. limbatus* | Indian Pass (29°40′8.05″N, 85°13′30.17″W), Gulf of Mexico, Florida | this study |
| Ingroup | *P. mattisi* n. sp. | PEET 461 | LRP 10115 | **MN686553** | | KC-7 | *C. limbatus* | west of Everglades (25°19.05′N, 82°29.76′W), Gulf of Mexico, Florida | this study |
| Ingroup | *P. mattisi* n. sp. | PEET 463 | LRP 10116 | **MN686554** | | MS05-435 | *C. limbatus* | St. Andrew Bay (30°8′4.69″N, 85°41′36.93″W), Panama City, Gulf of Mexico, Florida | this study |
| Ingroup | *P. mattisi* n. sp. | PEET 466 | LRP 10117 | **MN686555** | | MS05-457 | *C. brevipinna* | Horn Island (30°14′37.70″N, 88°46′37.62″W), Gulf of Mexico, Mississippi | this study |
| Ingroup | *P. mattisi* n. sp. | PEET 68 | LRP 10118 | | **MN659436** | TM-1 | *R. terraenovae* | Gulf of Mexico, Florida | this study |
| Ingroup | *P. mattisi* n. sp. | PEET 188 | LRP 10119 | | **MN659437** | MS05-24 | *C. limbatus* | Horn Island (30°14′37.70″N, 88°46′37.62″W), Gulf of Mexico, Mississippi | this study |
| Ingroup | *Paraorygmatobothrium orectolobi* (Butler, 1987) Ruhnke, 2011 | | no hologenophore | MG008940 | | | *Orectolobus maculatus* Bonnaterre | western Moreton Bay, Queensland, Australia | Cutmore et al. (2017) |

Table I. Continued.

| Ingroup/ Outgroup | Taxon | Specimen ID | Voucher accession no.* | GenBank accession no. (*28S rDNA*) | GenBank accession no. (*COI*) | Host accession no.† | Host species | Locality | Source |
|---|---|---|---|---|---|---|---|---|---|
| Ingroup | *P. orectolobi* | | no hologenophore | MG008941 | | | *Orectolobus ornatus* (De Vis) | western Moreton Bay, Queensland, Australia | Cutmore et al. (2017) |
| Ingroup | *Paraorygmatobothrium paulum* (Linton, 1897) Ruhnke, 2011 | PEET 454 | LRP 10120 | **MN686556** | | JL-6 | *G. cuvier* | off Montauk, Long Island Sound, New York | this study |
| Ingroup | *P. paulum* | | QM G232199 | HQ680628 | | | *G. cuvier* | off St. Helena Island, Moreton Bay, Queensland, Australia | Cutmore et al. (2011) |
| Ingroup | *P. paulum* | | QM G232200 | HQ680629 | | | *G. cuvier* | off St. Helena Island, Moreton Bay, Queensland, Australia | Cutmore et al. (2011) |
| Ingroup | *P. paulum* | | QM G232201 | HQ680630 | | | *G. cuvier* | off St. Helena Island, Moreton Bay, Queensland, Australia | Cutmore et al. (2011) |
| Ingroup | *Paraorygmatobothrium prionacis* (Yamaguti, 1934) Ruhnke, 1994 | PEET 459 | LRP 10121 | **MN686557** | | AI-4 | *Prionace glauca* (Linnaeus) | off Montauk, Long Island Sound, New York | this study |
| Ingroup | *P. prionacis* | TE-49 | LRP 8293 | KF685892 | | IF-7 | *P. glauca* | off Montauk, Long Island Sound, New York | Caira et al. (2014) |
| Ingroup | *Paraorygmatobothrium sinclairtaylori* Cutmore, Bennett, Miller, and Cribb, 2017 | | QM G233281 | MG008933 | | | *C. sorrah* | western Moreton Bay, Queensland, Australia | Cutmore et al. (2017) |
| Ingroup | *P. sinclairtaylori* | | QM G233307 | MG008934 | | | *Carcharhinus amboinensis* Müller and Henle | western Moreton Bay, Queensland, Australia | Cutmore et al. (2017) |
| Ingroup | *P. sinclairtaylori* | | QM G233318 | MG008935 | | | *C. leucas* | western Moreton Bay, Queensland, Australia | Cutmore et al. (2017) |
| Ingroup | *P. sinclairtaylori* | | no hologenophore | MG008936 | | | *Sphyrna mokarran* (Rüppell) | western Moreton Bay, Queensland, Australia | Cutmore et al. (2017) |
| Ingroup | *P. sinclairtaylori* | | QM G233329 | MG008937 | | | *Carcharhinus obscurus* Lesueur | western Moreton Bay, Queensland, Australia | Cutmore et al. (2017) |
| Ingroup | *P. sinclairtaylori* | PEET 469 | LRP 10122 | | **MN659438** | CM03-78 | *S. mokarran* | Weipa (12°35′11″S, 141°42′34″E), Gulf of Carpentaria, Queensland, Australia | this study |
| Ingroup | *Paraorygmatobothrium* sp. 1 sensu Cutmore et al. (2017) | | QM G233284 | MG008938 | | | *Carcharhinus cautus* Whitley | western Moreton Bay, Queensland, Australia | Cutmore et al. (2017) |
| Ingroup | *Paraorygmatobothrium* sp. 2 sensu Cutmore et al. (2017) | | QM G233298 | MG008932 | | | *S. lewini* | western Moreton Bay, Queensland, Australia | Cutmore et al. (2017) |
| Ingroup | *Paraorygmatobothrium* sp. 3 sensu Cutmore et al. (2017) | | QM G233338 | MG008926 | | | *C. amboinensis* | western Moreton Bay, Queensland, Australia | Cutmore et al. (2017) |

Table I. Continued.

| Ingroup/ Outgroup | Taxon | Specimen ID | Voucher accession no.* | GenBank accession no. (*28S rDNA*) | GenBank accession no. (*COI*) | Host accession no.† | Host species | Locality | Source |
|---|---|---|---|---|---|---|---|---|---|
| Ingroup | *Paraorygmatobothrium* sp. 3 sensu Cutmore et al. (2017) | | QM G233342 | MG008927 | | | *C. leucas* | western Moreton Bay, Queensland, Australia | Cutmore et al. (2017) |
| Ingroup | *Paraorygmatobothrium* sp. 4 sensu Cutmore et al. (2017) | | no hologenophore | MG008944 | | | *C. limbatus* | western Moreton Bay, Queensland, Australia | Cutmore et al. (2017) |
| Ingroup | *Paraorygmatobothrium taylori* Cutmore, Bennett, and Cribb, 2009 | | hologenophore not deposited | HQ680633 | | | *Hemigaleus australiensis* White, Last, and Compagno | off St. Helena Island, Moreton Bay, Queensland, Australia | Cutmore et al. (2011) |
| Ingroup | *P. taylori* | | QM G231307 | HQ680632 | | | *H. australiensis* | off St. Helena Island, Moreton Bay, Queensland, Australia | Cutmore et al. (2011) |
| Ingroup | *P. taylori* | | hologenophore not deposited | HQ680631 | | | *H. australiensis* | off St. Helena Island, Moreton Bay, Queensland, Australia | Cutmore et al. (2011) |
| Ingroup | *Paraorygmatobothrium typicum* (Subhapradha, 1955) Ruhnke, 2011 | PEET 124 | no hologenophore | | **MN659439** | BO-405 | *Rhizoprionodon* cf. *acutus* 3 | off Sarawak (02°49′01.20″N, 110°52′47.16″E), South China Sea, Malaysia | this study |
| Ingroup | *P. typicum* | PEET 125 | LRP 10123 | | **MN659440** | BO-405 | *R.* cf. *acutus* 3 | off Sarawak (02°49′01.20″N, 110°52′47.16″E), South China Sea, Malaysia | this study |
| Ingroup | *P. typicum* | PEET 310 | LRP 10124 | **MN686558** | **MN659441** | BO-402 | *R.* cf. *acutus* 3 | off Sarawak (02°49′01.20″N, 110°52′47.16″E), South China Sea, Malaysia | this study |
| Ingroup | *P. typicum* | PEET 311 | LRP 10125‡ | | **MN659442** | BO-402 | *R.* cf. *acutus* 3 | off Sarawak (02°49′01.20″N, 110°52′47.16″E), South China Sea, Malaysia | this study |
| Ingroup | *P. typicum* | PEET 312 | LRP 10126 | **MN686559** | **MN659443** | BO-405 | *R.* cf. *acutus* 3 | off Sarawak (02°49′01.20″N, 110°52′47.16″E), South China Sea, Malaysia | this study |
| Ingroup | *P. typicum* | PEET 313 | LRP 10127‡ | **MN686560** | **MN659444** | BO-405 | *R.* cf. *acutus* 3 | off Sarawak (02°49′01.20″N, 110°52′47.16″E), South China Sea, Malaysia | this study |
| Ingroup | *P. typicum* | PEET 314 | LRP 10128 | | **MN659445** | BO-405 | *R.* cf. *acutus* 3 | off Sarawak (02°49′01.20″N, 110°52′47.16″E), South China Sea, Malaysia | this study |
| Ingroup | *Paraorygmatobothrium ullmanni* Cutmore, Bennett, Miller, and Cribb, 2017 | | QM G233235 | MG008942 | | | *C. cautus* | western Moreton Bay, Queensland | Cutmore et al. (2017) |
| Ingroup | *P. ullmanni* | | QM G233239 | MG008943 | | | *C. amboinensis* | western Moreton Bay, Queensland | Cutmore et al. (2017) |
| Ingroup | *Ruhnkecestus latipi* Caira and Durkin, 2006 | TE-167 | LRP 8345 | KF685900 | | BO-265 | *Scoliodon macrorhynchos* Bleeker | off Sarawak, Malaysia | Caira et al. (2014) |

Table I. Continued.

| Ingroup/ Outgroup | Taxon | Specimen ID | Voucher accession no.* | GenBank accession no. (*28S rDNA*) | GenBank accession no. (*COI*) | Host accession no.† | Host species | Locality | Source |
|---|---|---|---|---|---|---|---|---|---|
| Ingroup | *Scyphophyllidium* cf. *giganteum* (van Beneden, 1858) Woodland, 1927 | TE-170 | LRP 8346 | KF685901 | | CR-140 | *Galeorhinus galeus* (Linnaeus) | Chatham Rise, New Zealand | Caira et al. (2014) |

* Hologenophore unless indicated otherwise.
† Additional host and locality data are available in the Global Cestode Database (http://elasmobranchs.tapewormdb.uconn.edu/) by searching on collection code (e.g., AU) and collection number (i.e., 30).
‡ Photo voucher.
§ Paragenophore.

v. 10.1.3. Sequences were aligned using webPRANK (Löytynoja and Goldman, 2010; https://www.ebi.ac.uk/goldman-srv/webprank/) using default settings, with the exception of the removal of the "+F" flag. Statistical selection of best-fit models of nucleotide substitution and maximum likelihood (ML) analyses were conducted through the CIPRES Science Gateway V3.3 portal (Miller et al., 2010; http://www.phylo.org/index.php). jModelTest2 on XSEDE (Guindon and Gascuel, 2003; Darriba et al., 2012) was used to estimate the best-fitting model of evolution. TVM+I+G was selected as a result of the evaluation of goodness of fit of 88 separate models based on corrected Akaike Information Criterion (AICc) values. One hundred separate ML analyses were performed using GARLI 2.0 on XSEDE (Zwickl, 2006). Default GARLI configurations settings were used with the following exceptions: "streefname = random," "attachmentspertaxon = 216" (i.e., twice the number of taxa included in the analysis to ensure all attachment points would be evaluated for each taxon), and "genthreshfortopoterm = 100,000" and "significanttopochange = 0.00001" for thorough exploration of tree space. Also in GARLI, 1,000 bootstrap replicates were performed to generate ML bootstrap values. Again, default GARLI configurations settings were used with the following exceptions: "streefname = random," "attachmentspertaxon = 216," and "genthreshfortopoterm = 10,000." Clades with bootstrap values of 95% or greater were considered to have high nodal support. SumTrees v. 4.0.0 in DendroPy v. 4.0.3 (Sukumaran and Holder, 2009) was used to summarize bootstrap support for clades onto the best tree resulting from the ML analyses.

In addition to the *28S rDNA* sequence data, *COI* sequence data were generated de novo in this study for the following 11 species of *Paraorygmatobothrium*: 7 specimens of *P. typicum*; 3 specimens of *P. arnoldi*; 2 specimens each of *Paraorygmatobothrium bai* Ruhnke and Carpenter, 2008, *P. christopheri*, and *P. exiguum*; 1 specimen each of *P. janineae* and *Paraorygmatobothrium sinclairtaylori* Cutmore, Bennett, Miller, and Cribb, 2017; and between 5 and 22 specimens of the new species described herein. Genomic DNA extraction, amplification protocols, PCR amplicon visualization, gel purification, DNA sequencing, and contiguous sequence assembly follow methods listed above for *28S rDNA*. *COI* amplification was achieved by using combinations of the following forward and reverse primers: forward primers Sean1 (5′-TTT ACT TTG GAT CAT AAG CG-3′), nLCO (5′-TTT ACT YTR GAY CAT AAG CGT-3′), reverse primers Ben1 (5′-RGT ACC AAA AAA CCA AAA CA-3′), Ben5 (5′-AAG CAG AAC CAA ATT TAC GAT C-3′), and Sean2 (5′-AAG CAG AAC CAA ATT TAC GAT-3′). The thermocycler temperature profile for the *COI* reaction was an initial incubation at 95 C for 2 min, denaturation at 95 C for 1 min, annealing at 47 C for 1 min, and extension at 72 C for 1 min for 50 cycles. The reaction was completed with a 5-min incubation at 72 C and then held indefinitely at 10 C. *COI* sequences of the 58 specimens of *Paraorygmatobothrium* were assembled into a matrix, aligned, and trimmed in Geneious v. 10.1.3. Genetic distances were calculated as the number of base pair differences, also in Geneious v. 10.1.3. Voucher accession numbers (for hologenophores, or, in 2 instances, paragenophores or photo vouchers), GenBank numbers, and host accession numbers, specimen IDs,

as well as host species and localities for all specimens for which *COI* sequence data were generated are also given in Table I.

## DESCRIPTIONS

### *Paraorygmatobothrium bullardi* n. sp.

(Figs. 1A, 2A–B, 3A–I)

*Description (based on 13 whole worms, 9 hologenophores, and 2 specimens observed with SEM):* Worms euapolytic, 9.3–13.8 (10.6 ± 1.4; 13) mm long; maximum width 285–680 (420 ± 138; 14) at level of scolex. Proglottids 17–34 (24 ± 5; 13) in number. Scolex consisting of 4 bothridia and cephalic peduncle, 228–470 (328 ± 81; 13) long by 285–680 (420 ± 139; 14) wide. Bothridia stalked, 214–380 (282 ± 49; 10; 15) long by 146–550 (241 ± 102; 14; 20) wide, with single loculus and apical sucker; stalks short; apical sucker 38–55 (49 ± 4; 18; 20) in diameter. Cephalic peduncle short. Neck 1.1–2.1 (1.7 ± 0.4; 11) mm long.

Distal bothridial surface covered with serrate gladiate spinitriches and papilliform to acicular filitriches, and columnar projections covered with papilliform to acicular filitriches (Fig. 3B, C). Proximal bothridial surface close to margin covered with serrate gladiate spinitriches and acicular to capilliform filitriches (Fig. 3D); gladiate spinitriches becoming less serrate and less dense more proximally (Fig. 3E). Bothridial rim covered with capilliform and acicular filitriches (Fig. 3C). Apex of scolex densely covered with capilliform filitriches (Fig. 3F). Cephalic peduncle covered with capilliform filitriches (Fig. 3G). Neck and strobila covered with capilliform filitriches (Fig. 3I) forming scutes (Fig. 3A, H).

Proglottids slightly craspedote. Posterior-most immature proglottids 442–1,320 (699 ± 312; 14) long by 200–530 (325 ± 85; 13) wide, length to width ratio 1.2–3.9:1 (2.3 ± 1; 12). Mature proglottids 1–4 (n = 15) in number; terminal mature proglottid 705–1,680 (1,259 ± 275; 20) long by 230–450 (312 ± 56; 20) wide, length to width ratio 2.1–6.9:1 (4.2 ± 1; 20). Gravid proglottids not observed. Testes 60–101 (80 ± 12; 19; 20) in number, 16–39 (28 ± 6; 19; 20) in number anterior to cirrus-sac, oblong, 20–80 (41 ± 18; 19; 24) long by 25–80 (55 ± 16; 19; 24) wide, in field anterior to ovary, arranged in 2–4 columns, 1 row deep. Cirrus-sac oval, 110–185 (149 ± 19; 19) long by 55–132 (86 ± 21; 18) wide, containing coiled cirrus. Cirrus armed with spinitriches. Vas deferens coiled, median, overlapping proximal portion of cirrus-sac, anterior to cirrus-sac. Genital pores lateral, irregularly alternating, 70–82% (76 ± 3.3; 20) of proglottid length from posterior end; genital atrium shallow. Vagina thin-walled, extending along median line anteriorly from Mehlis' gland to anterior extent of vas deferens then laterally along anterior margin of vas deferens entering genital atrium anterior to cirrus-sac. Ovary near posterior end of proglottid, H-shaped in frontal view, symmetrical, 150–360 (260 ± 60; 15) long by 130–270 (202 ± 38; 15) wide, tetralobed in cross section. Ovicapt 25–40 (34 ± 5; 12) in diameter, at posterior margin of ovarian bridge. Mehlis' gland posterior to ovicapt. Uterus ventral to vagina, extending from anterior margin of ovary to level of posterior margin of cirrus-sac. Uterine duct present, median, parallel and dorsal to uterus, enters uterus posterior to cirrus-sac. Eggs not seen. Vitellarium follicular; follicles 8–42 (16 ± 8; 20; 30) long by 8–45 (30 ± 11; 20; 29) wide, in 2 lateral fields each with 2–3 dorsal and 2–3 ventral columns of follicles, extending entire length of proglottid, interrupted by ovary and cirrus-sac. Excretory ducts in 2 lateral pairs.

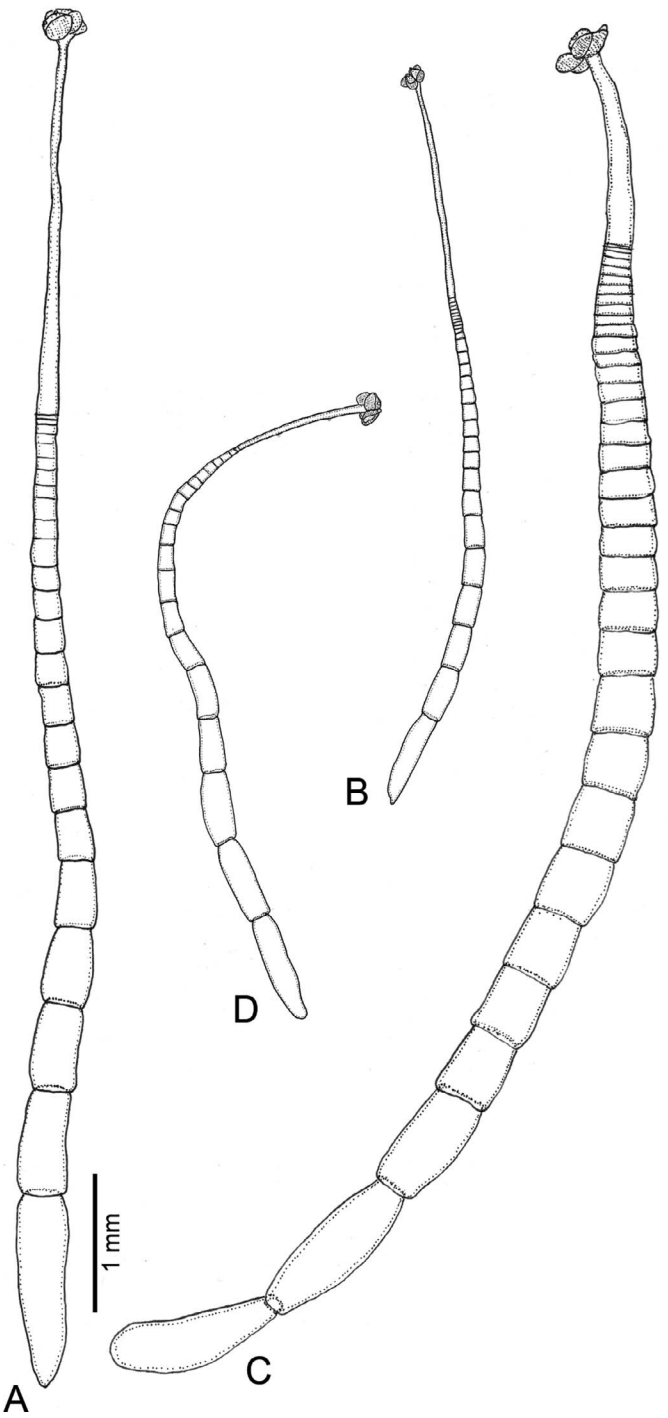


**Figure 1.** Line drawings (to scale) of whole worms of new species of *Paraorygmatobothrium*. (**A**) *Paraorygmatobothrium bullardi* n. sp. (holotype; USNM 1594951). (**B**) *Paraorygmatobothrium campbelli* n. sp. (holotype; USNM 1594959). (**C**) *Paraorygmatobothrium deburonae* n. sp. (holotype; USNM 1594967). (**D**) *Paraorygmatobothrium mattisi* n. sp. (holotype; USNM 1594975).

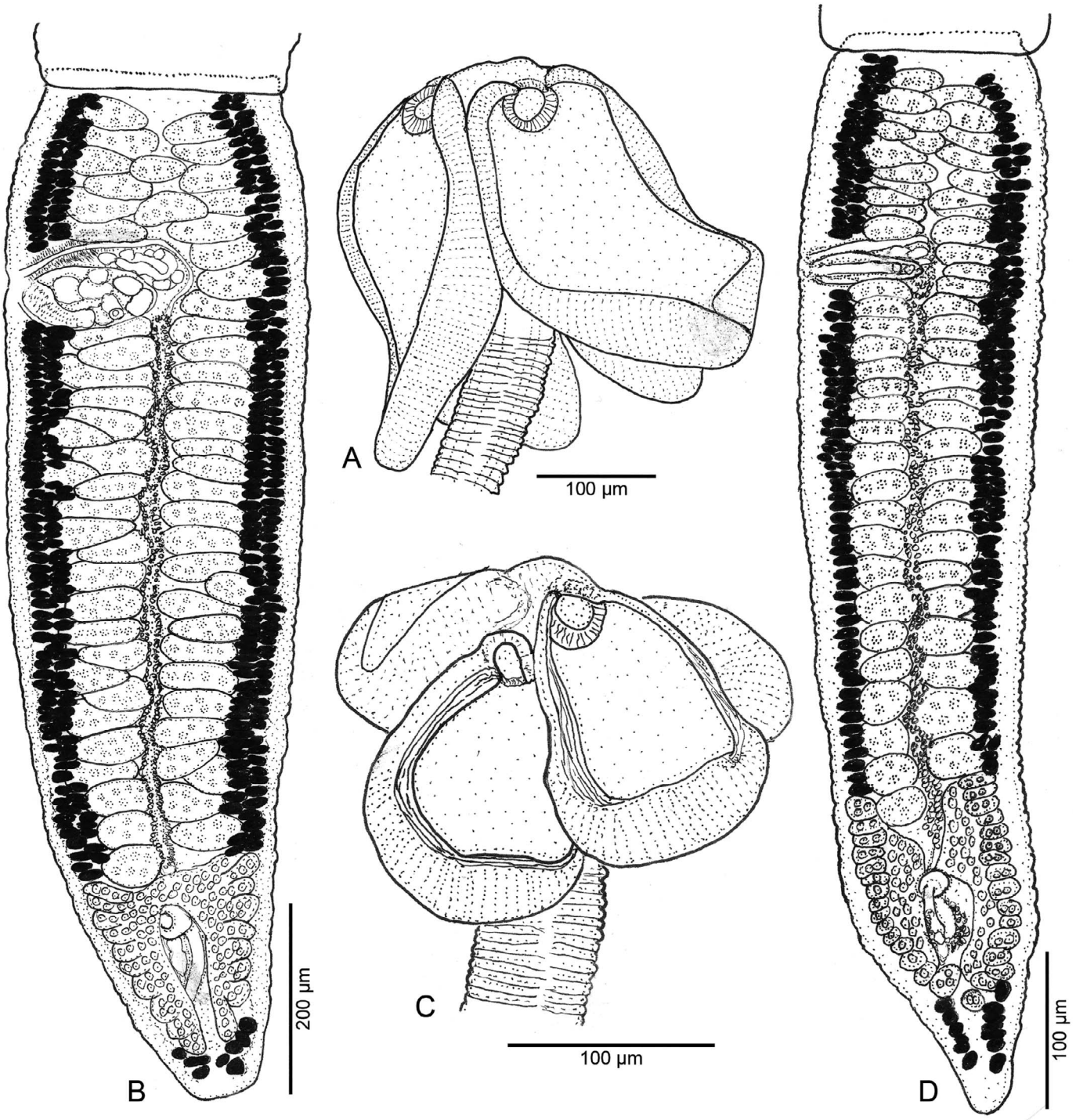


**Figure 2.** Line drawings of scolex and terminal proglottid of (**A, B**) *Paraorygmatobothrium bullardi* n. sp. and (**C, D**) *Paraorygmatobothrium campbelli* n. sp. (**A**) Scolex (paratype; LRP 7146). (**B**) Terminal, mature proglottid (paratype; LRP 7149). (**C**) Scolex (paratype; LRP 7191). (**D**) Terminal, mature proglottid (holotype; USNM 1594959).

## Taxonomic summary

*Type host: Carcharhinus brevipinna* (Müller and Henle), Spinner shark.

*Additional hosts: Carcharhinus acronotus* (Poey), Blacknose shark; *Carcharhinus limbatus* (Müller and Henle), Blacktip shark.

*Site of infection:* Spiral intestine.

*Type locality:* Gulf of Mexico, Mississippi, south of Shallow Fields (29°37′22.8″N, 88°30′11″W) (host no. MS05-5).

*Additional localities:* Gulf of Mexico, Florida, ~100 mi south of Tallahassee (28°37.15′N, 84°12.81′W) (*C. acronotus* [host no. KC-5]); Atlantic Ocean, Florida, off central Florida (28°0.8′N, 80°27′W) (*C. limbatus* [host no. DEL-8]); Gulf of Mexico,

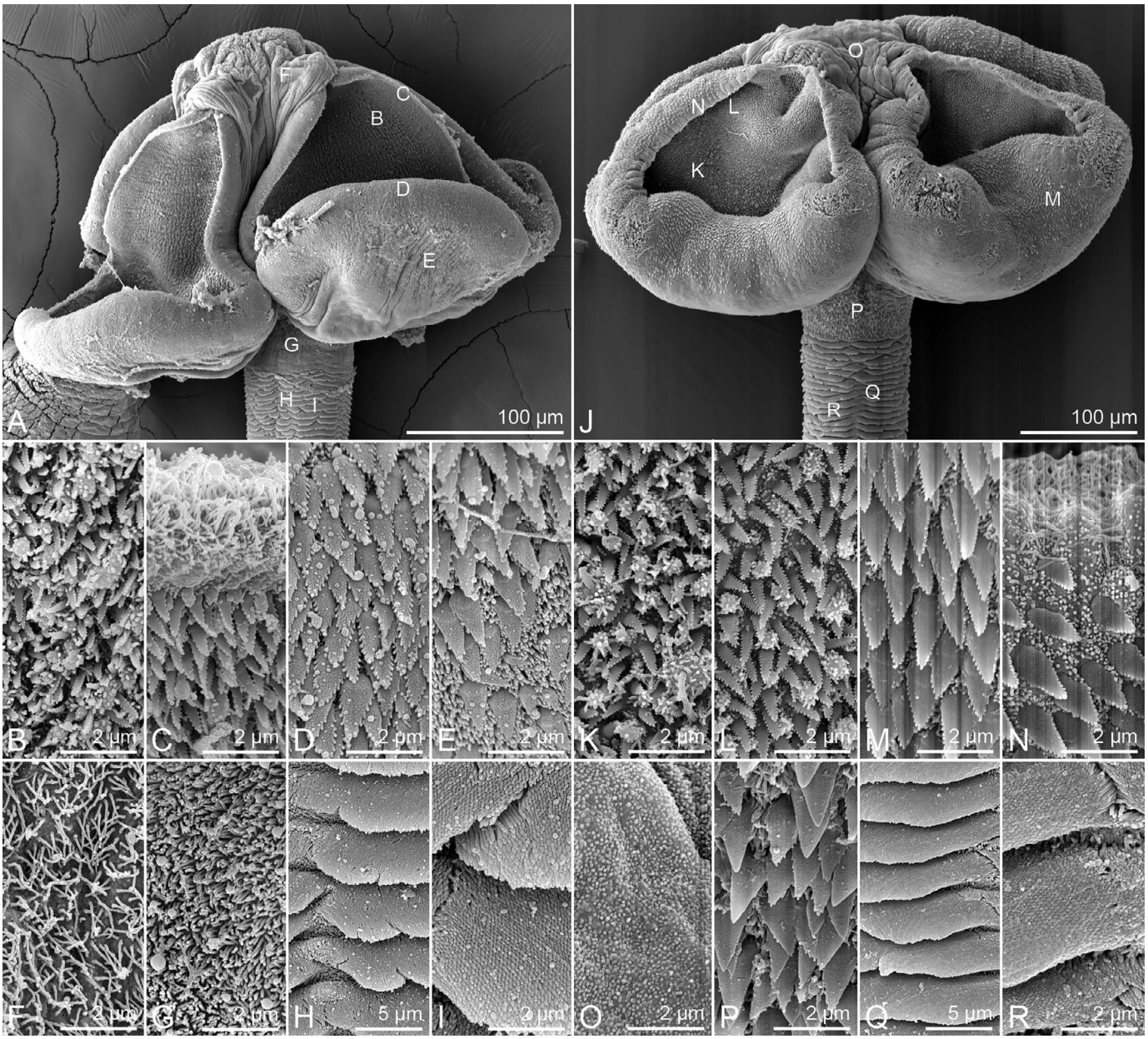


**Figure 3.** Scanning electron micrographs of (**A–I**) *Paraorygmatobothrium bullardi* n. sp. and (**J–R**) *Paraorygmatobothrium campbelli* n. sp. (**A**) Scolex; small letters indicate locations of details in B–I. (**B**) Distal bothridial surface. (**C**) Distal bothridial surface near rim. (**D**) Proximal bothridial surface close to margin. (**E**) Proximal bothridial surface away from margin. (**F**) Surface of scolex proper at apex of scolex. (**G**) Surface of cephalic peduncle. (**H**) Scutes. (**I**) Detail of scutes. (**J**) Scolex; small letters indicate locations of details in L–R. (**K**) Distal bothridial surface at center. (**L**) Distal bothridial surface near apical sucker. (**M**) Proximal bothridial surface. (**N**) Proximal bothridial surface near rim. (**O**) Surface of scolex proper at apex of scolex. (**P**) Surface of cephalic peduncle. (**Q**) Scutes. (**R**) Detail of scutes.

Florida, near oil rig MO-990 (29°58′58.20″N, 88°36′16.80″W) (*C. brevipinna* [host no. MS05-357]).

*ZooBank registration:* urn:lsid:zoobank.org:act:8EBE0D4C-12AC-4C41-9CF9-2E04E63B0BF6.

*Etymology:* This species is named for Dr. Ash Bullard of Auburn University in recognition of his skills and expertise in collecting the carcharhinid sharks from the Gulf of Mexico off Mississippi and Louisiana used in this study.

*Type specimens deposited:* Holotype (USNM 1594951), 7 paratypes (7 whole worms; USNM 1594952–1594958), 16 paratypes (5 whole worms [LRP 10060–10064], 9 hologenophores [LRP 7146–7149, 10067–10071], and 2 SEM vouchers [LRP 10065–10066]). Scoleces prepared for SEM retained in the collection of KJ at the University of Kansas.

## Remarks

Of the 21 species of *Paraorygmatobothrium* observed with scanning electron microscopy (SEM), *P. bullardi* differs in possession of serrate gladiate spinitriches as opposed to gongylate

columnar or gongylate gladiate spinitriches on the distal bothridial surfaces from *P. bai*, *Paraorygmatobothrium barberi* Ruhnke, 1993, *P. exiguum*, *Paraorygmatobothrium floraformis* (Southwell, 1912) Ruhnke, 2011, *Paraorygmatobothrium mobedii* Malek, Caira, and Haselii, 2010, *Paraorygmatobothrium rodmani* Ruhnke and Carpenter, 2008, *P. sinclairtaylori*, and *Paraorygmatobothrium sinuspersicense* Malek, Caira, and Haseli, 2010. Of the remaining 18 congeners, *P. bullardi* is longer than *P. arnoldi* and *P. typicum* (9.3–13.8 mm vs. 6.2–8.4 mm and 3.3–4.1 mm, respectively) and shorter than *Paraorygmatobothrium harti* Cutmore, Bennett, Miller, and Cribb, 2017, *Paraorygmatobothrium taylori* Cutmore, Bennett, and Cribb 2009, *Paraorygmatobothrium triacis* (Yamaguti, 1952) Ruhnke, 1996, and *Paraorygmatobothrium ullmani* Cutmore, Bennett, Miller, and Cribb, 2017 (9.3–13.8 mm vs. 14.2–18.4 mm, 25.9–32.9 mm, 35–46 mm, 14.8–24.8 mm, respectively). The apical sucker diameter of *P. bullardi* is smaller than that of *P. janineae, Paraorygmatobothrium leuci* (Watson and Thorson, 1976) Ruhnke, 2011, *Paraorygmatobothrium orectolobi* (Butler, 1987) Ruhnke, 2011, and *P. prionacis* (38–55 vs. 66–139, 68–82, 78–122, and 80–118, respectively), and it has fewer testes than *Paraorygmatobothrium kirstenae* Ruhnke, Healy, and Shapero, 2006 and *Paraorygmatobothrium musteli* (van Beneden, 1850) Ruhnke, 2011 (60–101 vs. 104–164 and 128–153, respectively). *Paraorygmatobothrium bullardi* differs from *Paraorygmatobothrium nicaraguensis* (Watson and Thorson, 1976) Ruhnke, 2011 in genital pore position (70–82% vs. 64–65% from posterior end of proglottid). *Paraorygmatobothrium bullardi* differs from *P. paulum* in lacking a conspicuous band of muscles along the locular periphery of the bothridia (see Ruhnke, 2011).

*Paraorygmatobothrium bullardi* is most similar to *Paraorygmatobothrium angustum* (Linton, 1889) Ruhnke, 2011, *P. christopheri*, *Paraorygmatobothrium filiforme* (Yamaguti, 1952) Ruhnke, 1996, and *Paraorygmatobothrium roberti* Ruhnke and Thompson, 2006. It can be distinguished from *P. christopheri* in lacking, rather than possessing, gladiate spinitriches on the cephalic peduncle, and from *P. filiforme* in possessing a slightly narrower scolex (261–425 vs. 430–530). While the ranges for the number of testes of *P. bullardi* and *P. roberti* overlap (60–101 vs. 82–141), the former species possesses 16–39 testes anterior to the cirrus-sac, while the latter can have as many as 64 testes anterior to the cirrus-sac (Ruhnke and Thompson, 2006; fig. 3). Last, while *P. bullardi* possesses a cephalic peduncle, *P. angustum* is reported to lack this feature (see Ruhnke, 2011). This species was referred to as *Paraorygmatobothrium* sp. 6 in Jensen and Bullard (2010).

## ***Paraorygmatobothrium campbelli* n. sp.**

(Figs. 1B, 2C–D, 3J–R)

*Description (based on 13 whole worms, 6 hologenophores, and 2 specimens observed with SEM):* Worms euapolytic, 2.5–5.6 (4 ± 1; 13) mm long; maximum width at level of scolex. Proglottids 15–23 (20 ± 3; 12) in number. Scolex consisting of 4 bothridia and cephalic peduncle, 122–180 (148 ± 23; 7) long by 150–251 (195 ± 26; 17) wide. Bothridia stalked, 100–180 (128 ± 24; 16; 22) long by 66–132 (105 ± 14; 18; 28) wide, with single loculus and apical sucker; stalks short; apical sucker 24–32 (29 ± 2; 17; 27) in diameter. Cephalic peduncle short. Neck 0.6–1.9 (1 ± 0.7; 6) mm long.

Distal bothridial surface covered with serrate gladiate spinitriches and papilliform to acicular filitriches, and columnar projections covered with papilliform to acicular filitriches (Fig. 3K, L). Proximal bothridial surface covered with serrate gladiate spinitriches and acicular filitriches (Fig. 3M); gladiate spinitriches becoming less dense more proximally and closer to the rim (Fig. 3N); papilliform instead of acicular filitriches near rim. Bothridial rim covered with capilliform filitriches (Fig. 3N). Apex of scolex covered with papilliform filitriches (Fig. 3O). Cephalic peduncle covered with gladiate spinitriches and capilliform filitriches (Fig. 3P); some gladiate spinitriches with sparse serrations. Neck and strobila covered with capilliform filitriches (Fig. 3R) forming scutes (Fig. 3J, Q).

Proglottids slightly craspedote. Posterior-most immature proglottids 260–420 (333 ± 50; 11) long by 120–220 (182 ± 33; 11) wide, length to width ratio 1.2–3.5:1 (1.9 ± 0.6; 11); terminal immature proglottids 440–950 (663 ± 230; 4) long by 125–270 (180 ± 45; 4) wide, length to width ratio 4–7.4:1 (5.6 ± 1.8; 4). Mature proglottids 0–2 (n = 16) in number; terminal mature proglottids 490–840 (672 ± 130; 12) long by 100–270 (180 ± 45; 12) wide, length to width ratio 2.5–6.2:1 (4 ± 1.1; 12). Gravid proglottids not observed. Testes 43–68 (56 ± 7; 18; 24) in number, 16–31(22 ± 4; 18; 24) in number anterior to cirrus-sac, oblong, 13–30 (22 ± 5; 11; 16) long by 24–67 (44 ± 12; 11; 16) wide, in field anterior to ovary, arranged in essentially 2 columns, 1 row deep. Cirrus-sac oval, 43–93 (77 ± 15; 11) long by 22–65 (35 ± 13; 11) wide, containing coiled cirrus. Cirrus armed with spinitriches. Vas deferens coiled, median, overlapping proximal portion of cirrus-sac, anterior to cirrus-sac. Genital pores lateral, irregularly alternating, 73–85% (78 ± 4; 12) of proglottid length from posterior end; genital atrium shallow. Vagina thin-walled, extending along median line anteriorly from Mehlis' gland to anterior extent of vas deferens then laterally along anterior margin of vas deferens entering genital atrium anterior to cirrus-sac. Ovary near posterior end of proglottid, H-shaped in frontal view, symmetrical, 58–148 (101 ± 29; 9) long by 35–125 (92 ± 27; 9) wide, tetralobed in cross section. Ovicapt 17–25 (21 ± 4; 3) in diameter, at posterior margin of ovarian bridge. Mehlis' gland posterior to ovicapt. Uterus ventral to vagina, extending from anterior margin of ovary to level of cirrus-sac. Uterine duct present, median, parallel and dorsal to uterus, enters uterus posterior to cirrus-sac. Eggs not seen. Vitellarium follicular; follicles 6–10 (7 ± 1; 7) long by 12–20 (15 ± 3; 7) wide, in 2 lateral fields each with essentially 1–2 dorsal and 1–2 ventral columns of follicles, extending entire length of proglottid, interrupted by ovary and cirrus-sac. Excretory ducts in 2 lateral pairs.

### Taxonomic summary

*Type and only host: Rhizoprionodon terraenovae* (Richardson), Atlantic sharpnose shark.

*Site of infection:* Spiral intestine.

*Type locality:* Atlantic Ocean, Florida, off Florida (29°35.38′N, 80°32.3′W) (host no. DEL-13).

*Additional localities:* Gulf of Mexico, Mississippi, Horn Island (30°14′37.70″N, 88°46′37.62″W) (host no. MS05-23) and Horn Island (30°14′14.33″N, 88°46′25.12″W) (host no. MS05-550); Atlantic Ocean, South Carolina, Wadmalaw Point (32°37′45.84″N, 80°16′02.26″W), North Edisto River (host no. CH-8).

*ZooBank registration:* urn:lsid:zoobank.org:act:0FFE10DD-E738-4526-A843-9727E43F440A.

*Etymology:* This species is named in honor of Dr. William Campbell in recognition of his noted contributions to parasitology and particular fondness for fancifully portraying elasmobranch tapeworms.

*Type specimens deposited:* Holotype (USNM 1594959), 7 paratypes (7 whole worms; USNM 1594960–1594966), 13 paratypes (5 whole worms [LRP 10072–10076], 6 hologenophores [LRP 7189–7192, 10079–10080], and 2 SEM vouchers [LRP 10077–10078]). Scoleces prepared for SEM retained in the collection of KJ at the University of Kansas.

*Additional specimens deposited:* Hologenophore (LRP 10081).

## Remarks

*Paraorygmatobothrium campbelli* differs from the existing 27 species in the genus except for *P. angustum*, *P. arnoldi*, *P. exiguum*, *P. floraformis*, *P. paulum*, *P. roberti*, *P. sinuspersicense*, and *P. typicum* in possessing either a smaller or larger total length. The species is easily distinguished from *P. angustum*, *P. arnoldi*, *P. exiguum*, *P. paulum*, and *P. roberti* in possessing a smaller apical sucker (24–32 vs. 42–55, 40–54, 50–85, 43–68, 43–68, respectively). While *P. campbelli* possesses serrate gladiate spinitriches on the distal bothridial surface, *P. floraformis* and *P. sinuspersicense* possess gongylate columnar spinitriches on that surface. *Paraorygmatobothrium campbelli* is most similar to *P. typicum*. However, *P. campbelli* can be distinguished from *P. typicum* in that it is euapolytic rather than hyperapolytic. Of the 16 specimens in the type series of *P. campbelli*, 12 possessed either 1 or 2 mature proglottids, while the remainder were immature worms. This species was referred to as *Paraorygmatobothrium* sp. 2 in Jensen and Bullard (2010).

## ***Paraorygmatobothrium deburonae* n. sp.**

(Figs. 1C, 4A–B, 5A–H)

*Description (based on 14 whole worms, 18 hologenophores, and 2 specimens observed with SEM):* Worms slightly euapolytic, 7.5–16.3 (11.1 ± 2.6; 14) mm long; maximum width 277–570 (408 ± 81; 23) at level of scolex. Proglottids 30–44 (35 ± 4; 10) in number. Scolex consisting of 4 bothridia and cephalic peduncle, 215–425 (310 ± 57; 18) long by 277–570 (408 ± 81; 23) wide. Bothridia stalked, 174–390 (266 ± 52; 23; 33) long by 148–310 (216 ± 43; 23; 35) wide, with single loculus and apical sucker; stalks short; apical sucker 45–78 (54 ± 9; 17; 21) in diameter. Cephalic peduncle short. Neck 1.1–3.2 (2.2 ± 0.8; 7) mm long.

Distal bothridial surface covered with gongylate gladiate spinitriches and papilliform to acicular filitriches (Fig. 5B, C). Proximal bothridial surface covered with serrate gladiate spinitriches and acicular filitriches (Fig. 5D). Bothridial rim covered with capilliform filitriches (Fig. 5E). Apex of scolex densely covered with acicular filitriches (Fig. 5F). Microtriches on cephalic peduncle not observed. Neck and strobila covered with capilliform filitriches (Fig. 5H) forming scutes (Fig. 5A, G).

Proglottids slightly craspedote. Posterior-most immature proglottids 432–700 (531 ± 85; 23) long by 264–525 (418 ± 75; 23) wide, length to width ratio 0.9–1.8:1 (1.3 ± 0.3; 22); terminal immature proglottids 760–1,030 (n = 2) long by 250–410 (n = 2) wide, length to width ratio 1.9–4.1:1 (n = 2). Mature proglottids 0–6 (n = 27) in number; terminal mature proglottids 838–2,160 (1,225 ± 289; 25) long by 240–780 (416 ± 111; 25) wide, length to width ratio 1.7–5.9:1 (3.1 ± 1; 22). Gravid proglottids not observed. Testes 71–111 (88 ± 10; 31; 39) in number, 26–54 (36 ± 7; 31; 39) in number anterior to cirrus-sac, oblong, 25–70 (40 ± 12; 22; 32) long by 25–75 (56 ± 12; 22; 32) wide, in field anterior to ovary, arranged in 4–6 irregular columns, 1 row deep. Cirrus-sac oval, 130–269 (180 ± 35; 21) long by 50–143 (91 ± 30; 21) wide, containing coiled cirrus. Cirrus armed with spinitriches. Vas deferens coiled, median, overlapping proximal portion of cirrus-sac, anterior to cirrus-sac. Genital pores lateral, irregularly alternating, 53–85% (72 ± 8; 18) of proglottid length from posterior end. Vagina thin-walled, extending along median line anteriorly from Mehlis' gland to anterior extent of vas deferens then laterally along anterior margin of vas deferens entering genital atrium anterior to cirrus-sac. Ovary near posterior end of proglottid, H-shaped in frontal view, symmetrical, 210–420 (314 ± 66; 17) long by 145–365 (268 ± 66; 17) wide, tetralobed in cross section. Ovicapt 30–55 (41 ± 8; 8) in diameter, at posterior margin of ovarian bridge. Mehlis' gland posterior to ovicapt. Uterus ventral to vagina, extending from anterior margin of ovary to level of cirrus-sac. Uterine duct present, median, parallel and dorsal to uterus, enters uterus posterior to cirrus-sac. Eggs not seen. Vitellarium follicular; follicles 10–23 (16 ± 4; 15; 27) long by 16–50 (36 ± 9; 15; 27) wide, in 2 lateral fields each with 2–4 dorsal and 2–4 ventral columns of follicles, extending entire length of proglottid, interrupted by ovary and cirrus-sac. Excretory ducts in 2 lateral pairs.

## Taxonomic summary

*Type host: Carcharhinus isodon* (Müller and Henle), Finetooth shark.

*Additional hosts: Carcharhinus brevipinna* (Müller and Henle), Spinner shark; *Carcharhinus limbatus* (Müller and Henle), Blacktip shark; *Rhizoprionodon terraenovae* (Richardson), Atlantic sharpnose shark.

*Site of infection:* Spiral intestine.

*Type locality:* Gulf of Mexico, Mississippi, Round Island (30°17′42.45″N, 88°35′11.55″W) (host nos. MS05-83 and MS05-86).

*Additional localities:* Gulf of Mexico, Florida, Indian Pass (29°40′8.05″N, 85°13′30.17″W) (*C. limbatus* [host nos. MS05-482, MS05-484, MS05-488–491]; *C. isodon* [host no. MS05-495 and MS05-496]); Gulf of Mexico, Mississippi, Horn Island (30°14′37.70″N, 88°46′37.62″W) (*R. terraenovae* [host no. MS05-21]; *C. limbatus* [host no. MS05-24]) and south of Shallow Fields (29°37.38″N, 88°30′11″W) (host no. MS05-4); Atlantic Ocean, South Carolina, Bulls Bay (*C. limbatus* [host no. CH-48]; *C. isodon* [host no. CH-49]).

*ZooBank registration:* urn:lsid:zoobank.org:act:0D6772FE-31D5-43D1-ABF4-97A648EF920F.

*Etymology:* This species is named for Dr. Isaure de Buron in gratitude for providing KJ and her students with the lab space needed to collect tapeworms from carcharhinid sharks off South Carolina.

*Type specimens deposited:* Holotype (USNM 1594967), 7 paratypes (7 whole worms; USNM 1594968–1594974), 26 paratypes (6 whole worms [LRP 10085–10090], 18 hologenophores [LRP 7144–7145, 7160, 7162–7164, 7174–7175, 7177, 7196–7197, 10093–10099], and 2 SEM vouchers [LRP 10091–

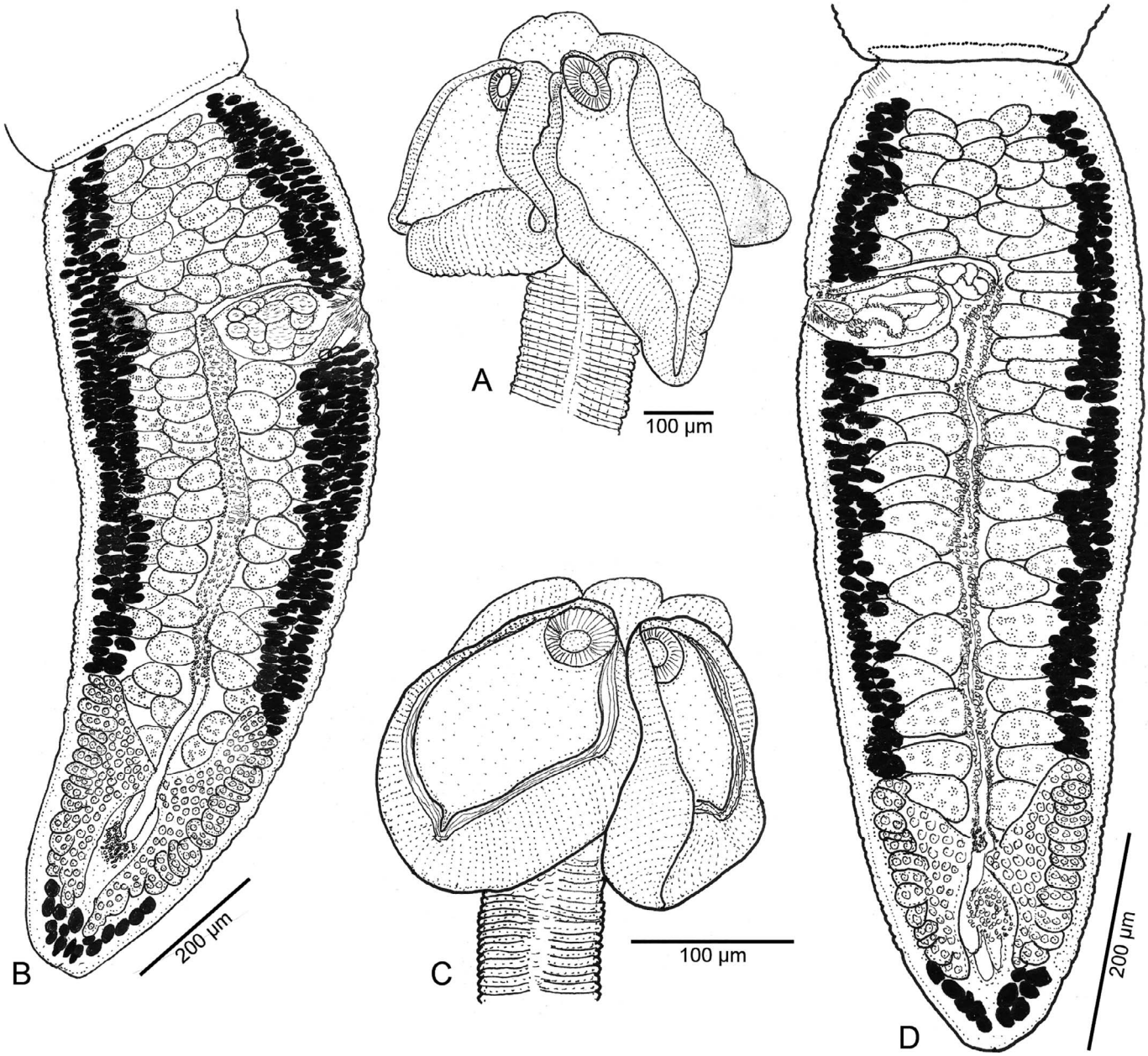


**Figure 4.** Line drawings of scolex and terminal proglottid of (**A, B**) *Paraorygmatobothrium deburonae* n. sp. and (**C, D**) *Paraorygmatobothrium mattisi* n. sp. (**A**) Scolex (paratype; LRP 7162). (**B**) Terminal, mature proglottid (paratype; LRP 7162). (**C**) Scolex (paratype; LRP 7143). (**D**) Terminal, mature proglottid (paratype; LRP 7193).

10092]). Scoleces prepared for SEM retained in the collection of KJ at the University of Kansas.

*Additional specimens deposited:* Eight hologenophores (LRP 7158–7159, 7161, 7165, 7176, 7178, 7198, 10100).

## Remarks

Of the 23 species of *Paraorygmatobothrium* observed with SEM (of 28 species total), *P. deburonae* differs from all but *P. barberi* in possessing gongylate gladiate spinitriches on the distal bothridial surfaces rather than either gongylate columnar or serrate gladiate spinitriches on this surface. It differs from *P. barberi* and *P. triacis* in its shorter total length (7.5–16.3 vs. 20–36 and 35–46, respectively). Of the remaining 4 species, *P. deburonae* differs from *P. leuci* in possessing vitelline follicles arranged in 2–4 dorsal and 2–4 ventral columns rather than in 1–2 dorsal and 1–2 ventral columns, from *P. nicaraguensis* in possessing a greater number of proglottids (30–44 vs. 24–25), and from *P. musteli* in possessing fewer testes (71–111 vs. 128–153). *Paraorygmatobothrium deburonae* is most similar to *P. filiforme* in all counts and measurements but differs from this species in possessing rather than lacking a cephalic peduncle. This species was referred to as *Paraorygmatobothrium* sp. 5 in Jensen and Bullard (2010).

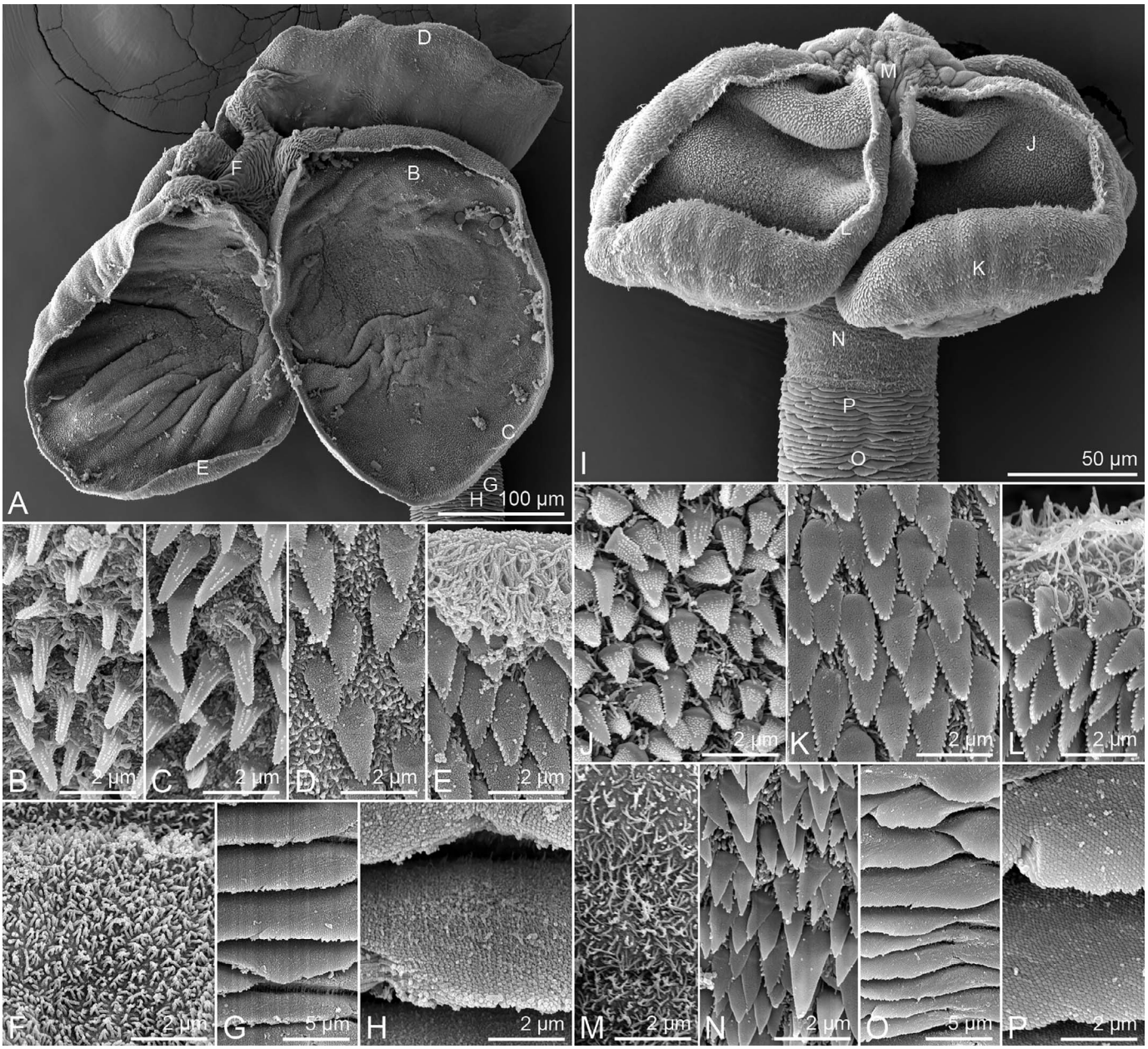


**Figure 5.** Scanning electron micrographs of (**A–H**) *Paraorygmatobothrium deburonae* n. sp. and (**I–P**) *Paraorygmatobothrium mattisi* n. sp. (**A**) Scolex; small letters indicate locations of details in B–H. (**B**) Distal bothridial surface. (**C**) Distal bothridial surface near rim. (**D**) Proximal bothridial surface. (**E**) Proximal bothridial surface near rim. (**F**) Surface of scolex proper at apex of scolex. (**G**) Scutes. (**H**) Detail of scutes. (**I**) Scolex; small letters indicate locations of details in **J–P**. (**J**) Distal bothridial surface. (**K**) Proximal bothridial surface. (**L**) Proximal bothridial surface near rim. (**M**) Surface of scolex proper at apex of scolex. (**N**) Surface of cephalic peduncle. (**O**) Scutes. (**P**) Detail of scutes.

### ***Paraorygmatobothrium mattisi* n. sp.**

(Figs. 1D, 4C–D, 5I–P)

*Description (based on 15 whole worms, 12 hologenophores, and 3 specimens observed with SEM):* Worms euapolytic, 3.4–8 (4.9 ± 1.2; 14) mm long; maximum width 210–396 (281 ± 53; 23) at level of scolex. Proglottids 13–23 (19 ± 3; 14) in number. Scolex consisting of 4 bothridia and cephalic peduncle, 140–318 (209 ± 47; 22) long by 210–396 (281 ± 53; 23) wide. Bothridia stalked, 120–317 (191 ± 41; 36) long by 108–245 (151 ± 29; 36) wide, with single loculus and apical sucker; stalks short; apical sucker 25–50 (35 ± 6; 22; 33) in diameter. Cephalic peduncle short. Neck 0.5–1.0 (0.8 ± 0.2; 8) mm long.

Distal bothridial surface covered with gongylate gladiate spinitriches and papilliform to acicular filitriches (Fig. 5J). Proximal bothridial surface covered with serrate gladiate spinitriches and acicular to capilliform filitriches (Fig. 5K, L). Bothridial rim covered with capilliform filitriches (Fig. 5L). Apex of scolex densely covered with acicular to capilliform filitriches (Fig. 5M). Cephalic peduncle covered with gladiate spinitriches of varying sizes and capilliform filitriches (Fig. 5N); some gladiate

spinitriches with serrations. Neck and strobila covered with capilliform filitriches (Fig. 5P) forming scutes (Fig. 5I, O).

Proglottids slightly craspedote. Posterior-most immature proglottids 375–996 (521 ± 153; 18) long by 169–284 (224 ± 34; 18) wide, length to width ratio 1.4–4.1:1 (2.4 ± 0.7; 18); terminal immature proglottids 560–690 (611 ± 60; 4) long by 175–250 (207 ± 34; 4) wide, length to width ratio 2.2–3.9:1 (3 ± 0.8; 4). Mature proglottids 0–3 (n = 24) in number; terminal mature proglottids 560–1,953 (965 ± 281; 21) long by 165–446 (219 ± 68; 21) wide, length to width ratio 3.2–6.8:1 (4.5 ± 0.9; 20). Gravid proglottids not observed. Testes 47–100 (67 ± 12; 27; 33) in number, 18–45 (26 ± 6; 27; 33) in number anterior to cirrus-sac, oblong, 13–64 (33 ± 14; 19; 28) long by 14–102 (45 ± 20; 19; 28) wide in field anterior to ovary, arranged in 2–4 columns, 1 row deep. Cirrus-sac oval, 70–198 (109 ± 30; 16) long by 32–171 (60 ± 32; 16) wide, containing coiled cirrus. Cirrus armed with spinitriches. Vas deferens coiled, median, overlapping proximal portion of cirrus-sac, anterior to cirrus-sac. Genital pores lateral, irregularly alternating, 72–80% (76 ± 3; 16) of proglottid length from posterior end; genital atrium shallow. Vagina thin-walled, extending along median line anteriorly from Mehlis' gland to anterior extent of vas deferens then laterally along anterior margin of vas deferens entering genital atrium anterior to cirrus-sac. Ovary near posterior end of proglottid, H-shaped in frontal view, symmetrical, 78–392 (193 ± 77; 14) long by 45–210 (115 ± 39; 14) wide, tetralobed in cross section. Ovicapt 22–35 (27 ± 5; 8) in diameter, at posterior margin of ovarian bridge. Mehlis' gland posterior to ovicapt. Uterus ventral to vagina, extending from anterior margin of ovary to level of anterior margin of cirrus-sac. Uterine duct present, median, parallel and dorsal to uterus, enters uterus posterior to cirrus-sac in posterior proglottids. Eggs not seen. Vitellarium follicular; follicles 8–25 (13 ± 5; 6; 19) long by 6–30 (20 ± 9; 6; 19) wide, in 2 lateral fields each with 2–3 dorsal and 2–3 ventral columns of follicles, extending entire length of proglottid, interrupted by ovary and cirrus-sac. Excretory ducts in 2 lateral pairs.

## Taxonomic summary

*Type host: Rhizoprionodon terraenovae* (Richardson), Atlantic sharpnose shark.

*Additional hosts: Carcharhinus brevipinna* (Müller and Henle), Spinner shark; *Carcharhinus limbatus* (Müller and Henle), Blacktip shark.

*Site of infection:* Spiral intestine.

*Type locality:* Gulf of Mexico, Mississippi, Horn Island (30°14′37.70″N, 88°46′37.62″W) (*R. terraenovae* [host nos. MS05-21], *C. limbatus* [host no. MS05-24], and *C. brevipinna* [host no. MS05-457]).

*Additional localities:* Gulf of Mexico, Florida, St. Andrew Bay (30°8′4.69″N, 85°41′36.93″W), Panama City (*C. limbatus* [host no. 435]), west of Everglades (25°19.05′N, 82°29.76′W) (*C. limbatus* [host no. KC-7]), Indian Pass (29°40′8.05″N, 85°13′30.17″W) (*C. limbatus* [host nos. MS05-488 and MS05-490]), and off Florida (*R. terraenovae* [host no. TM-1]).

*ZooBank registration:* urn:lsid:zoobank.org:act:4BE9451F-1C28-4719-8EA8-AFF44C5CF0A6.

*Etymology:* This species is named in honor of the late Dr. Tom Mattis in recognition of his knowledge about elasmobranch tapeworm biology.

*Type specimens deposited:* Holotype (USNM 1594975), 9 paratypes (9 whole worms; USNM 1594976–1594984), 20 paratypes (5 whole worms [LRP 10105–10109], 12 hologenophores [LRP 7142–7143, 7172–7173, 7193–7195, 10113–10117], and 3 SEM vouchers [LRP 10110–10112]). Scoleces prepared for SEM retained in the collection of KJ at the University of Kansas.

*Additional specimens deposited:* Two hologenophores (LRP 10118–10119).

## Remarks

Of the 24 species of *Paraorygmatobothrium* observed with SEM (of 29 species total), *P. mattisi* differs from all but *P. barberi* and *P. deburonae* in possessing gongylate gladiate spinitriches on the distal bothridial surfaces rather than either gongylate columnar or serrate gladiate spinitriches. *Paraorygmatobothrium mattisi* differs from both of these species in possessing fewer proglottids (13–23 vs. 47–67 and 30–44, respectively). Of the remaining 5 species, *Paraorygmatobothrium mattisi* can be distinguished from *P. filiforme, P. leuci, P. nicaraguensis,* and *P. triacis* in being a smaller worms (3.4–8 mm in total length vs. 11.8–23.7 mm, 10.1–42 mm, 9.5–22 mm, and 35–46 mm, respectively) and from *P. musteli* in possessing fewer testes (47–100 vs. 128–153). This species was referred to as *Paraorygmatobothrium* sp. 3 in Jensen and Bullard (2010).

## Phylogenetic analysis and genetic distance data

The phylogenetic analysis was based on partial (D1–D3) *28S rDNA* sequence data alone; *COI* sequence data were used to assess inter- versus intra-specific sequence variation (see below). The number of base pairs (bp) of *28S rDNA* sequence data generated de novo for the 34 specimens of *Paraorygmatobothrium* ranged from 581 bp to 891 bp; 892 bp were generated de novo for the outgroup species *Hemipristicola gunterae*. Among the 108 specimens included in the analysis, unaligned sequence length ranged from 581 to 1,214 bp after sequences were cropped to minimize missing data. Alignment using webPrank resulted in a matrix 1,228 bp in length. The phylogenetic tree resulting from the ML analysis with bootstrap nodal support values is shown in Figure 6.

The ingroup taxa, comprising the 4 new species of *Paraorygmatobothrium*, 18 additional species in the genus (i.e., 14 previously named species and 4 undescribed species characterized by Cutmore et al. [2017] based on molecular data), and 7 other phyllobothriidean species representing 6 genera, were recovered as monophyletic, albeit with low support. Not unexpectedly, the 4 new species were not recovered as each other's closest relatives. *Paraorygmatobothrium bullardi* placed as the sister taxon to *Paraorygmatobothrium* sp. 3 of Cutmore et al. (2017) with strong support, in a clade that also included a taxon referred to by Caira et al. (2014) as belonging to *Marsupiobothrium* Yamaguti, 1952, as the earliest diverging lineage. *Paraorygmatobothrium campbelli* was found in a strongly supported clade with *P. christopheri*, *P. typicum,* and *Ruhnkecestus latipi* Caira and Durkin, 2006. This clade in turn placed as sister to a clade including *Paraorygmatobothrium* sp. 2 of Cutmore et al. (2017), and a strongly supported *P. mattisi* and *P. sinclairtaylori* as each other's closest relatives. Finally, *P. deburonae* placed as member of a clade also including *Doliobothrium* sp., *Paraorygmatobothrium* sp. 1 of Cutmore, *P. arnoldi*, and *P. harti*. With respect to the genus as

a whole, species of *Paraorygmatobothrium* were not recovered as monophyletic with respect to one another, with species of *Doliobothrium* Caira, Malek, and Ruhnke, 2011, *Marsupiobothrium* sp., *Nandocestus* Reyda, 2008, *Orectolobicestus* Ruhnke, Caira, and Carpenter, 2006, *Ruhnkecestus* Caira and Durkin, 2006, *Scyphophyllidium* Woodland, 1927, placing amongst the species of *Paraorygmatobothrium* (see Fig. 6).

Alignment of *COI* sequence data resulted in a matrix 448 bp in length. Within species, *COI* sequence variation was lowest among the 2 specimens each of *P. bai* and *P. christopheri* (i.e., 0 bp) and the 3 specimens of *P. arnoldi* (i.e., 0–2 bp), and largest among the 22 specimens of *P. deburonae* (i.e., 0–11 bp) and the 7 specimens of *P. mattisi* (i.e., 0–8 bp) (Table II). Inter-specific *COI* sequence variation ranged from 21 to 24 bp between *P. mattisi* and *P. sinclairtaylori* to 78–80 bp between *P. arnoldi* and *P. janineae*. The amount of *COI* sequence divergence was relatively uniform across the new species and ranged from 46 to 58 bp for *P. campbelli* as compared to *P. mattisi* to 72–77 bp for *P. bullardi* as compared to *P. campbelli*.

## DISCUSSION

With the description of the 4 new species in this paper, the number of species of *Paraorygmatobothrium* expands to 30. There is a strong possibility that this number represents only a fraction of the actual species diversity, as sampling of individual candidate carcharhiniform host species has revealed a number of undescribed species. For example, analysis of *28S rDNA* and *ND1* mtDNA by Cutmore et al. (2017) revealed evidence of 4 undescribed species of *Paraorygmatobothrium*. Sequence analysis of *ND1* by T. R. Ruhnke (unpubl. data) has thus far revealed an additional 5 undescribed species that are genetically distinct from all those included in the phylogenetic analysis in this study.

Collectively, species of *Paraorygmatobothrium* have been reported to possess either serrate gladiate or gongylate columnar spinitriches on their distal bothridial surfaces (see Ruhnke, 2011). Here we report on a third form of spinitriches, gongylate gladiate spinitriches (see Fig. 5B, C, J), found on the distal bothridial surfaces of *P. deburonae* and *P. mattisi*. While Chervy (2009; fig. 2) provided comprehensive terminology to allow us to name this new type of microthrix, Chervy did not explicitly report on microtriches of this type. Re-examination of SEMs presented for *P. barberi* (see Ruhnke, 1994; fig. 34), showed this species to also possess this new type of microthrix. While Ruhnke (1994) described the distal bothridial surfaces of *P. barberi* to be covered with "microtriches resembling an 'ear of corn'" (p. 73) (i.e., gongylate columnar in Ruhnke [2011]), these spinitriches appear to be flat (i.e., oval in cross section) rather than circular in cross section, thus considered to be gladiate spinitriches here.

As species of *Paraorygmatobothrium* have been added to the literature, difficulty in distinguishing them based solely on morphological comparison has been encountered. Cutmore et al. (2017) noted difficulty in assessing species assignments with respect to *P. sinclairtaylori* and *Paraorygmatobothrium* sp. 3 via comparative analysis of their morphologies. This issue was compounded by the fact that both species were found to parasitize Pigeye shark, *Carcharhinus amboinensis* (Müller and Henle), and the Bull shark, *Carcharhinus leucas* (Müller and Henle). However, their analysis of *28S rDNA* and *ND1* mtDNA provided clear delineation of these 2 species. Our description of *P. bullardi, P. campbelli, P. deburonae*, and *P. mattisi* confirms the concerns of Cutmore et al. (2017) regarding reliance on morphological features solely for the delineation of species of *Paraorygmatobothrium* complicated by the fact that multiple species of *Paraorygmatobothrium* parasitize the same host species or even the same host specimen. For example, *P. campbelli*, *P. deburonae*, and *P. mattisi* parasitize *R. terraenovae*, and *P. bullardi*, *P. deburonae,* and *P. mattisi* also parasitize *C. limbatus*. At a minimum, both *P. deburonae* and *P. mattisi* were found parasitizing 3 of the same host individuals (i.e., a specimen of *R. terraenovae* [MS05-21] and 2 specimens of *C. limbatus* [MS05-24 and MS05-490]). The 4 new tapeworm species described herein could only be distinguished from one another by combinations of subtle, non-unique features, with a general trend being that *P. campbelli* and *P. mattisi* are smaller species, and *P. bullardi* and *P. deburonae* are larger species (see Fig. 1). Analysis of *28S rDNA* sequence data (Fig. 6), supported by *COI* distances (Table II), reveals that specimens of *Paraorygmatobothrium* from their carcharhinid hosts from the Gulf of Mexico and the Atlantic Ocean are clearly genetically distinct species (Fig. 6). For example, the 7 specimens of *P. bullardi* differ from one another in 0–5 bp in 448 bp of *COI* generated, but differed from *P. campbelli* by 72–77 bp, from *P. deburonae* by 66–74 bp, and from *P. mattisi* by 64–74 bp (see Table II). In general, the within-species *COI* divergence for species of *Paraorygmatobothrium* was less than 10% of the between-species divergence among these 4 species. In addition, ultrastructural features in the form of scolex microthrix pattern were particularly useful in distinguishing the 4 species from one another, and from other congeners. *Paraorygmatobothrium bullardi* and *P. campbelli* possess serrate gladiate spinitriches on their distal bothridial surfaces (Fig. 3B, C and Fig. 3K, L, respectively), while *P. deburonae* and *P. mattisi* sport gongylate gladiate spinitriches on their distal bothridial surfaces (Fig. 5B, C and Fig. 5J, respectively). The latter is a microthrix shape *P. deburonae* and *P. mattisi* share with only *P. barberi*. This study underscores the need to include molecular sequence data and ultrastructural features, in addition to traditional morphological and anatomical features, in distinguishing among species of *Paraorygmatobothrium*.

Given the difficulties in using morphology to delineate species of *Paraorygmatobothrium*, in addition to the more catholic host association for many species of the genus, care should be taken in terms of proceeding with the description of species. In this study, we quantified scolex morphology and proglottid anatomy for all hologenophores for which such data could be assessed. Moreover, study series for the 4 new species were assembled from whole worms and hologenophore, often from the same host specimens. For example, the type series of *P. mattisi* comprises whole worms from host individuals from which some of the hologenophores (also in the type series) were collected (i.e., *C. limbatus* specimen MS05-24 and *R. terraenovae* specimen MS05-21). We recommend this approach for future descriptions of new species of *Paraorygmatobothrium*.

Phylogenetic analysis of *28S rDNA* sequence data revealed interesting preliminary geographic patterns of the relationships for 3 of the 4 new species of *Paraorygmatobothrium*. Rather than the 4 species forming a clade, each species was closely related to species of *Paraorygmatobothrium* parasitizing sharks from Australia and Borneo (see Fig. 6). *Paraorygmatobothrium bullardi* was the sister taxon to *Paraorygmatobothrium* sp. 3 of Cutmore et al.

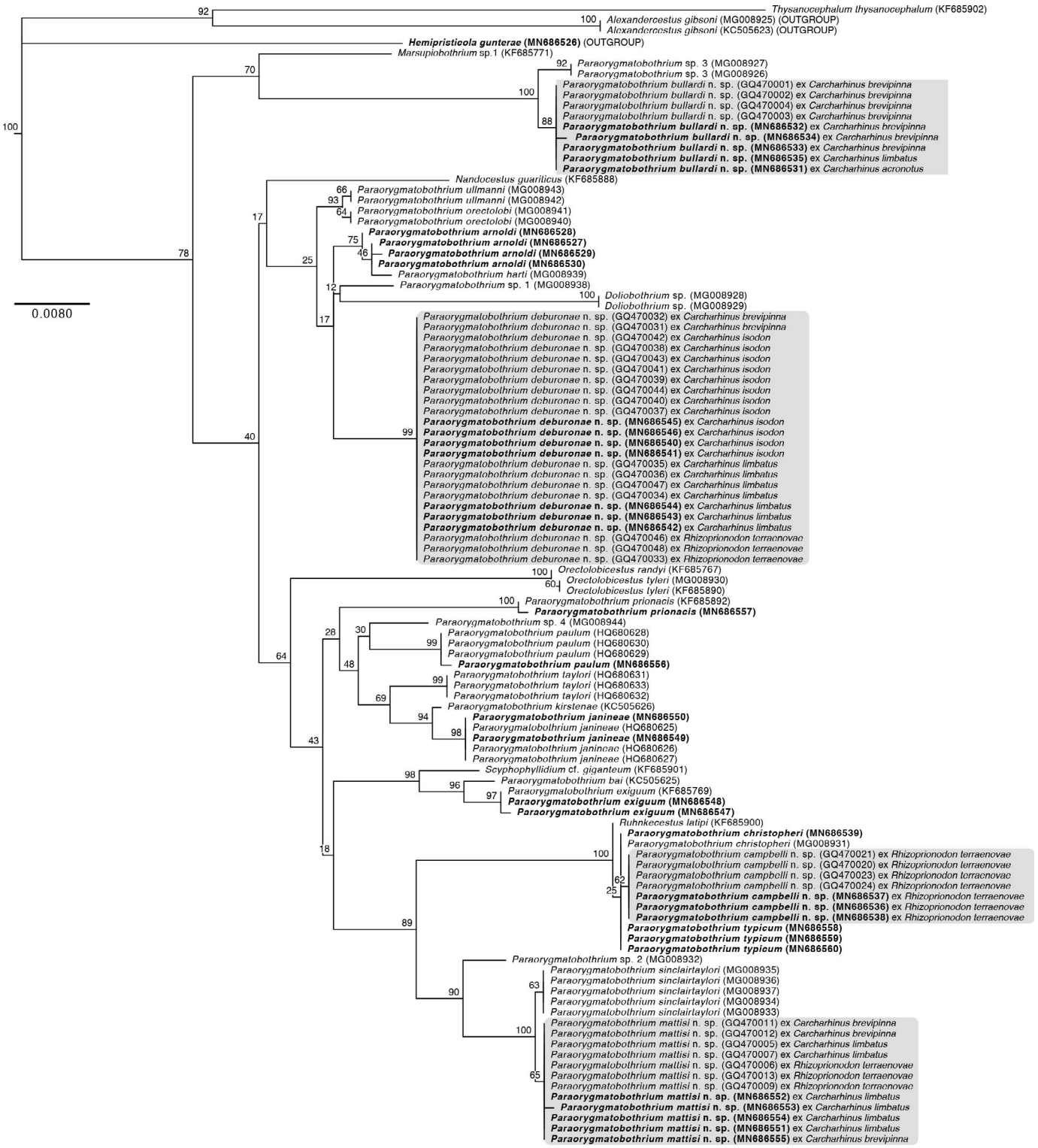


**Figure 6.** Best maximum likelihood topology resulting from phylogenetic analysis of combined partial (D1–D3) *28S rDNA* sequence data of species of *Paraorygmatobothrium* and related genera showing phylogenetic placement of new species of *Paraorygmatobothrium* (indicated by grey boxes). Taxon labels include species name, GenBank accession numbers (in parentheses), and host species; labels of specimens for which sequence data were generated as part of this study given in bold. Nodal support given as bootstrap (BS) values generated from 1,000 BS replicates. Branch length scale bar at lower left indicates nucleotide substitutions per site.

**Table II.** Distance matrix (number of differences) of 448 bp of COI sequence data of selected species of *Paraorygmatobothrium*, including new species.

| | *Paraorygmatobothrium arnoldi* | *Paraorygmatobothrium bai* | *Paraorygmatobothrium bullardi* n. sp. | *Paraorygmatobothrium campbelli* n. sp. | *Paraorygmatobothrium christopheri* | *Paraorygmatobothrium deburonae* n. sp. | *Paraorygmatobothrium exiguum* | *Paraorygmatobothrium janineae* | *Paraorygmatobothrium mattisi* n. sp. | *Paraorygmatobothrium sinclairtaylori* | *Paraorygmatobothrium typicum* |
|---|---|---|---|---|---|---|---|---|---|---|---|
| *Paraorygmatobothrium arnoldi* (n = 3) | 0–2 | 72–73 | 74–76 | 71–74 | 62–70 | 69–74 | 67–69 | 78–80 | 69–74 | 73 | 74–77 |
| *Paraorygmatobothrium bai* (n = 2) | | 0 | 72–75 | 70–71 | 63–65 | 69–74 | 56–57 | 60 | 59–67 | 61 | 64–67 |
| *Paraorygmatobothrium bullardi* n. sp. (n = 6) | | | 0–5 | 72–77 | 65–71 | 66–74 | 68–72 | 69–71 | 64–74 | 71–73 | 61–64 |
| *Paraorygmatobothrium campbelli* n. sp. (n = 5) | | | | 1–5 | 33–37 | 63–69 | 49–52 | 57–59 | 46–58 | 59–61 | 37–40 |
| *Paraorygmatobothrium christopheri* (n = 2) | | | | | 0 | 52–65 | 39–43 | 57–58 | 42–52 | 51 | 30–34 |
| *Paraorygmatobothrium deburonae* n. sp. (n = 22) | | | | | | 0–11 | 62–69 | 64–68 | 55–67 | 66–71 | 54–62 |
| *Paraorygmatobothrium exiguum* (n = 2) | | | | | | | 3 | 63–64 | 52–62 | 62–64 | 46–50 |
| *Paraorygmatobothrium janineae* (n = 1) | | | | | | | | — | 63–74 | 68 | 56–57 |
| *Paraorygmatobothrium mattisi* n. sp. (n = 7) | | | | | | | | | 0–8 | 21–24 | 41–56 |
| *Paraorygmatobothrium sinclairtaylori* (n = 1) | | | | | | | | | | — | 49–52 |
| *Paraorygmatobothrium typicum* (n = 7) | | | | | | | | | | | 0–5 |

(2017) from the *C. amboinensis* and *C. leucas* from Australia. *Paraorygmatobothrium campbelli* was found in a clade with *P. christopheri* from the Spot-tail shark, *Carcharhinus sorrah* (Müller and Henle) from Australia and *P. typicum* from 1 of the Milk sharks, *Rhizoprionodon* cf. *acutus* 3 (sensu Naylor et al., 2012), from Borneo. *Paraorygmatobothrium mattisi* was the sister taxon to *P. sinclairtaylori* parasitizing several species of *Carcharhinus* Blainville and a species of hammerhead shark from Australia. Given that only 18 of the 30 described species of *Paraorygmatobothrium* were included in the phylogenetic analysis, a formal investigation of geographic patterns will require more comprehensive taxonomic and geographic sampling.

Prior to 2010, species of *Paraorygmatobothrium* had been reported to exhibit oioxenous specificity (sensu Euzet and Combes, 1980). Strict host specificity is generally the case for non-trypanorhynchan species of elasmobranch tapeworms (see Caira and Jensen, 2014) with few exceptions (see, e.g., Tyler and Caira, 1999; Reyda et al., 2016; Dedrick et al., 2018). Molecular sequence data from Jensen and Bullard (2010) first indicated that strict host specificity might not be the rule in *Paraorygmatobothrium*. Most recently, Cutmore et al. (2017) reported on 12 species of *Paraorygmatobothrium*. They described 4 of these species as new, 4 were known species, and 4 were left undescribed. Three of these species, *P. orectolobi, P. ullmanni*, and *Paraorygmatobothrium* sp. 3 were referred to as having low host specificity (i.e., parasitizing 2 host species in a single shark genus), and a fourth, *P. sinclairtaylori*, was listed as exhibiting euryxenous host specificity (i.e., parasitizing as many as 5 host species in 2 shark families). Based on revised host associations for *Paraorygmatobothrium* sp. 6 of Jensen and Bullard (2010) (now *P. bullardi*) to include *C. limbatus* and *C. acronotus* as hosts, here we reiterate a metastenoxenic pattern of host specificity for *P. mattisi* and *P. deburonae* (i.e., species parasitizing more than 1 genus of host, but the hosts are restricted to a single family; sensu Caira et al., 2003) and report a mesostenoxenic pattern of host specificity for *P. bullardi* (i.e., species parasitizing more than 1 congener of host; sensu Caira et al., 2003); only *P. campbelli* appears to exhibit oioxenous host specificity. In all likelihood, the examples of more relaxed host specificity for species of *Paraorygmatobothrium* have been discovered because of these more comprehensive collections of shark hosts in relatively defined geographic areas (i.e., the Gulf of Mexico [Jensen and Bullard, 2010] and Moreton Bay, Australia [Cutmore et al., 2017]). It is highly likely that strict host specificity will be found to be violated in other species of *Paraorygmatobothrium* when a more comprehensive collection of candidate hosts and more broadscale geographic collections are completed.

Caira et al. (2014) and Cutmore et al. (2017) found *Paraorygmatobothrium* to be paraphyletic with respect to other phyllobothriidean genera. Given that the same locus and nearly identical taxon representation as that of Cutmore et al. (2017) were used herein, albeit with increased specimen sampling for the target species, their results are confirmed: species of *Doliobothrium*, *Nandocestus*, *Orectolobicestus*, *Ruhnkecestus*, and *Scyphophyllidium* group among species of *Paraorygmatobothrium*. The case of *Paraorygmatobothrium* and related phyllobothriideans presents a difficult problem from a standpoint of where taxonomy meets morphological patterns. As noted by Cutmore et al. (2017), species of *Paraorygmatobothrium* share a conserved pattern of morphological features (i.e., simple, undivided bothridia with an apical sucker; proximal bothridial surfaces covered with serrate, gladiate spinitriches; most mature proglottids that are longer than wide; post-vaginal testes; and vitelline follicles arranged in 2 lateral fields; also see Ruhnke, 2011). However, some phyllobothriid genera that are closely related to subsets of species of

*Paraorygmatobothrium* also share distinctive features with the latter genus. For example, the proglottids of *Orectolobicestus* and *Ruhnkecestus latipi* are remarkably similar in morphology to those of species of *Paraorygmatobothrium* (see Ruhnke et al., 2006; Caira and Durkin, 2006) but differ in autapomorphies of scolex morphology (marginal loculi in *Orectolobicestus* and facial loculi in *Ruhnkecestus*). *Scyphophyllidium* cf. *giganteum* (van Beneden, 1858) Woodland, 1927 is also nested among species of *Paraorygmatobothrium* (see Fig. 6), but this species is relatively dissimilar in scolex and proglottid morphology (see Ruhnke, 2011). We heartily concur with the sentiments of Cutmore et al. (2017) that a taxonomic solution is needed to address the widespread paraphyly of *Paraorygmatobothrium* with respect to the other genera.

## ACKNOWLEDGMENTS

We are grateful to Janine Caira (University of Connecticut [UConn]) for valuable discussions during the preparation of the manuscript. We thank Ash Bullard (Auburn University), Jody Peterson, Eric Hoffmayer (Gulf Coast Research Laboratory [GCRL], University of Southern Mississippi), and Robin Overstreet (GCRL) for logistical support and collections of carcharhinid sharks off Mississippi and Louisiana; Dana Bethea, Lisa Hollensead, and Megan Winton (National Marine Fisheries Service, Panama City, Florida) for collections of carcharhinid sharks off Florida; Bryan Frazier and Ashley Shaw (South Carolina Department of Natural Resources), and Isaure de Buron (College of Charleston) for logistical support and collections of carcharhinid sharks off South Carolina; and NOAA Fisheries for providing opportunity for KJ to collect tapeworms from carcharhinid sharks aboard the R.V. *Oregon II* and *Delaware II* in 1996 and 2001, respectively. We thank Amber Moore (West Virginia State University [WVSU]) for assistance in measuring the new species of *Paraorygmatobothrium*; Robin Turner and Chase Turner (both WVSU) for generating *COI* sequence data for several samples; Gopinath Venkata Vajja (WVSU) for providing ABI 3130 analysis for *28S rDNA* and *COI*; and Seth Bollinger (University of Kansas [KU]) for assistance with specimen preparation. Scott Cutmore (University of Queensland) is thanked for providing information on species and specimens of *Paraorygmatobothrium* from Australia. We further thank Joanna Cielocha, Hannah Owens, Rachel Guyer, and Kaylee Herzog (KU) for assistance with the collection of tapeworms in South Carolina and Florida. We are grateful to Eduardo Rosa-Molinar and Noraida Martinez-Rivera (Microscopy Analytical Imaging Resource Core Laboratory, KU) for providing access to and support for using the Hitachi SU8320 Cold Field Emission scanning electron microscope, and Kaylee Herzog (KU) for her SEM assistance. Janine Caira (Lawrence R. Penner Parasitology Collection, UConn) is thanked for providing a multitude of loans. We also thank 2 anonymous reviewers for their comments that helped improve the manuscript. This research was supported with funds from West Virginia NASA REA awards, a Kansas EPSCoR First Award, NSF PBI awards DEB 0818696 and 0818823, and NSF Phylogenetic Systematics awards DEB 1457762 and 1457776, and DEB 1921404 and 1921411. Any opinions, findings, and conclusions or recommendations here are those of the authors and do not necessarily reflect the views of the National Science Foundation.

## LITERATURE CITED

Benson, D. A., I. Karsch-Mizrachi, D. J. Lipman, J. Ostell, and D. L. Wheeler. 2005. GenBank. Nucleic Acids Research 33: D34–D38.

Caira, J. N., and S. M. Durkin. 2006. A new genus and species of tetraphyllidean cestode from the spadenose shark, *Scoliodon laticaudus*, in Malaysian Borneo. Comparative Parasitology 73: 42–48.

Caira, J. N., and K. Jensen. 2014. A digest of elasmobranch tapeworms. Journal of Parasitology 100: 373–391.

Caira, J. N., K. Jensen, and E. Barbeau (eds.). 2018. Global Cestode Database. Available at: http://elasmobranchs.tapewormdb.uconn.edu/. Accessed 15 July 2019.

Caira, J. N., K. Jensen, and K. E. Holsinger. 2003. On a new index of host specificity. *In* Taxonomie, Écologie et Évolution des Métazoaires Parasites. (Livre Hommage à Louis Euzet). Tome 1, C. Combes and J. Jourdane (eds.). PUP, Perpignan, France, p. 161–201.

Caira, J. N., K. Jensen, A. Waeschenbach, P. D. Olson, and D. T. J. Littlewood. 2014. Orders out of chaos—Molecular phylogenetics reveals the complexity of shark and stingray tapeworm relationships. International Journal for Parasitology 44: 55–73.

Chervy, L. 2009. Unified terminology for cestode microtriches: A proposal from the International Workshops on Cestode Systematics in 2002–2008. Folia Parasitologica 56: 199–230.

Cutmore, S. C., M. B. Bennett, T. L. Miller, and T. H. Cribb. 2017. Patterns of specificity and diversity in species of *Paraorygmatobothrium* Ruhnke, 1994 (Cestoda: Phyllobothriidae) in Moreton Bay, Queensland, Australia, with the description of four new species. Systematic Parasitology 94: 941–970.

Cutmore, S. C., S. M. Theiss, M. B. Bennett, and T. H. Cribb. 2011. *Hemipristicola gunterae* gen. n., sp. n. (Cestoda: Tetraphyllidea: Phyllobothriidae) from the snaggletooth shark, *Hemipristis elongata* (Carcharhiniformes: Hemigaleidae), from Moreton Bay, Australia. Folia Parasitologica 58: 187–196.

Darriba, D., G. L. Taboada, R. Doallo, and D. Posada. 2012. jModelTest 2: More models, new heuristics and parallel computing. Nature Methods 9: 772.

Dedrick, E. A., F. B. Reyda, E. K. Iwanyckyj, and T. R. Ruhnke. 2018. Two new species of *Stillabothrium* (Cestoda: Rhinebothriidea) from stingrays of the genus *Fontitrygon* from Senegal. Folia Parasitologica 65: 014. doi:10.14411/fp.2018.014.

Euzet, L., and C. Combes. 1980. Les problèms de l'espèce chez les animaux parasites. Memoires Societe Zoologique de France 40: 239–285.

Guindon, S., and O. Gascuel. 2003. A simple, fast, and accurate algorithm to estimate large phylogenies by maximum likelihood. Systematic Biology 52: 696–704.

Herzog, K. S., and K. Jensen. 2017. A new genus with two new species of lecanicephalidean tapeworms (Cestoda) from the mangrove whipray, *Urogymnus granulatus* (Myliobatiformes: Dasyatidae) from the Solomon Islands and northern Australia. Folia Parasitologica 64: 004. doi:10.14411/fp.2017.004.

Jensen, K., and S. A. Bullard. 2010. Characterization of a diversity of tetraphyllidean and rhinebothriidean cestode larval types, with comments on host associations and life-cycles. International Journal for Parasitology 40: 889–910.

Löytynoja, A., and N. Goldman. 2010. webPRANK: A phylogeny-aware multiple sequence aligner with interactive alignment browser. BMC Bioinformatics 11: 579.

Miller, M. A., W. Pfeiffer, and T. Schwartz. 2010. Creating the CIPRES Science Gateway for inference of large phylogenetic trees. 2010 Gateway Computing Environments Workshop (GCE), New Orleans, Louisiana, p. 1–8.

Naylor, G. J. P., J. N. Caira, K. Jensen, K. A. M. Rosana, W. T. White, and P. R. Last. 2012. A DNA sequence–based approach to the identification of shark and ray species and its implications for global elasmobranch diversity and parasitology. Bulletin of the American Museum of Natural History 367: 1–262.

Pleijel, F., U. Jondelius, E. Norlinder, A. Nygren, B. Oxelman, C. Schander, P. Sundberg, and M. Thollesson. 2008. Phylogenies without roots? A plea for the use of vouchers in molecular phylogenetic studies. Molecular Phylogenetics and Evolution 48: 369–371.

Reyda, F., C. Healy, A. Haslach, T. Ruhnke, T. Aprill, M. Bergman, A. Daigler, E. Dedrick, I. Delgado, K. Forti, et al. 2016. A new genus of rhinebothriidean cestodes from batoid elasmobranchs, with the description of five new species and two new combinations. Folia Parasitologica 63: 038. doi:10.14411/fp.2016.038

Ruhnke, T. R. 1994. *Paraorygmatobothrium barberi* n. g., n. sp. (Cestoda: Tetraphyllidea), with amended descriptions of two species transferred to the genus. Systematic Parasitology 28: 65–79.

Ruhnke, T. R. 2011. A monograph on the Phyllobothriidae (Platyhelminthes, Cestoda). Bulletin of the University of Nebraska State Museum 25: 1–208.

Ruhnke, T. R., J. N. Caira, and S. D. Carpenter. 2006. *Orectolobicestus* n. g. (Cestoda: Tetraphyllidea), with the description of five new species and the transfer of *Phyllobothrium chiloscyllii* to the new genus. Systematic Parasitology 65: 215–233.

Ruhnke, T. R., J. N. Caira, and A. Cox. 2015. The cestode order Rhinebothriidea no longer family-less: A molecular phylogenetic investigation with erection of two new families and description of eight new species of *Anthocephalum*. Zootaxa 3904: 51–81.

Ruhnke, T. R., and V. A. Thompson. 2006. Two new species of *Paraorygmatobothrium* (Tetraphyllidea: Phyllobothriidae) from the lemon sharks *Negaprion brevirostris* and *Negaprion acutidens* (Carcharhiniformes: Carcharhinidae). Comparative Parasitology 73: 35–41.

Ruhnke, T. R., and R. E. Workman. 2013. Two new species and a new phyllobothriid cestode genus from sharks of the genus *Negaprion* Whitley (Carcharhiniformes). Systematic Parasitology 85: 37–48.

Sukumaran, J., and M. T. Holder. 2009. DendroPy Phylogenetic Computing Library Version 3.0.0. Available at: http://dendropy.org. Accessed 15 September 2019.

Tyler, G. A., and J. N. Caira. 1999. Two new species of *Echinobothrium* (Cestoidea: Diphyllidea) from myliobatiform elasmobranchs in the Gulf of California, Mexico. Journal of Parasitology 85: 327–335.

Zwickl, D. J. 2006. Genetic algorithm approaches for the phylogenetic analysis of large biological sequence datasets under the maximum likelihood criterion. Doctoral Dissertation. University of Texas at Austin, Austin, Texas, 125 p.